

The Unsteady Cavity in Internal Flows

Thesis by

Jong Hyun Kim

In Partial Fulfillment of the Requirements

for the Degree of
Doctor of Philosophy

California Institute of Technology
Pasadena, California

1971

(Submitted May 26, 1971)

Acknowledgements

With all my utmost sincerity, I would like to thank my thesis advisor, Professor Allan J. Acosta, for his unique and brilliant guidance and supervision that helped bring this work to a successful completion. His ungrudging criticisms, comments and many valuable suggestions that originated from his supreme professional insight invariably inspired me. Also his continued encouragement, great tolerance and patience during the hours of numerous discussions on both academic and personal problems are especially appreciated.

Thanks are also due to the California Institute of Technology which provided me with the scholarships throughout the full course of this study.

Deep and sincere appreciation goes to Mrs. Julie Powell for her excellent typing and careful preparation of the manuscript, and to Miss Cecilia Lin who did all the drawings.

Also it is a pleasure for me to confess that the constant encouragement of my wife Jungshuh and all my family was the freshening source of my energy during this work.

Abstract

The problems of the two-dimensional unsteady cavity in internal flow are treated and linear theories are developed. In Part I, the two-dimensional supercavitating flow past a flat plate heaving and pitching with small amplitudes in a choked tunnel is investigated and a linearized solution is obtained using the acceleration potential. The flat plate is inclined at a small angle of attack to the oncoming flow and the cavity pressure is assumed to be constant. Force and moment coefficients are calculated for the case of the foil placed in the middle of the walls as functions of reduced frequency and the ratio of tunnel height to chord length. The pressure disturbances caused by the unsteady motion of the foil do not die out far upstream; these also depend on the chord-tunnel height ratio and reduced frequency.

Another type of cavity problem in an internal flow is studied in Part II. Here, the finite cavity flow over a wedge held stationary in the middle of a tunnel is investigated. A salient feature of the problem is that the mass oscillation is allowed. Also the pressure on the cavity is allowed to vary in a prescribed manner. The problem is linearized using the complex perturbation velocity and the formal solution is obtained. The choked case in the presence of the overall mass fluctuation is obtained as a limiting case. Throughout the analysis, it is assumed that the change of the cavity length with time is small.

Table of Contents

	<u>Page</u>
Acknowledgements	ii
Abstract	iii
Nomenclature	vi
General Introduction	1
Part I. The Wall Effect for Unsteady, Choked Supercavitating Flow	7
1. Introduction	8
2. Formulation of the Problem	9
3. Solution of the Boundary Value Problem	13
4. Pressure at Infinity, Force and Moment	24
5. Formulation of an Equivalent Problem	27
6. Numerical Results and Discussion	29
7. Conclusion	34
References	35
Appendices	38
Table and Figures	46
Part II. The Cavitating Internal Flow with Mass Oscillations	54
1. Introduction	55
2. Formulation of the Problem	56
3. Solution of the Boundary Value Problem	60
4. Discussion and Conclusion	74

	<u>Page</u>
Part II. (continued)	
References	78
Figures	81

Nomenclature

\vec{a}	acceleration vector
C_f	normal force coefficient
\tilde{C}_f	amplitude of the unsteady part of C_f
C_{F_r}	normalized component of \tilde{C}_f in phase with the apparent change in the angle of attack
C_{F_i}	quadrature counterpart of C_{F_r}
C_m	moment coefficient about the leading edge of the foil (tail up positive)
\tilde{C}_m	amplitude of the unsteady part of C_m
C_{M_r}	normalized component of \tilde{C}_m in phase with the apparent change in the angle of attack
C_{M_i}	quadrature counterpart of C_{M_r}
$F(z, t)$	complex acceleration potential
$g(\xi)$	function defined in Equation (25)
h_1	distance between the foil and the upper wall
h_2	distance between the foil and the lower wall
h	distance between the foil and the walls when $h_1 = h_2$; also distance between the wedge and the walls
H	homogeneous solution for complex acceleration potential; and for complex perturbation velocity in Part II
i	unit imaginary number with regard to space

j	unit imaginary number with respect to time, $i \cdot j \neq -1$
J_1, J_2, J_{3a} J_{4a}, J_{3b}, J_{4b}	} integrals
k	reduced frequency, ω/U
$l(t)$	cavity length in Part II
P	pressure
$P(\zeta)$	a rational function
\vec{q}	velocity vector
$Q(x)$	a function characteristic of the motion of the foil
$S(t)$	cavity end point in transformed plane in Part II
t	time
u	dimensionless perturbation velocity in the x-direction; also dimensioned perturbation velocity in the x-direction in Part II
v	dimensionless perturbation velocity in the y-direction; also dimensioned perturbation velocity in the y-direction in Part II
U	velocity at upstream infinity
x, y	coordinates in physical plane
z	complex variable in the linearized physical plane
Y	ordinate of the foil; also ordinate of the cavity surface in Part II
$W(z)$	complex perturbation velocity for steady flow in Part I; also unsteady complex perturbation velocity in Part II

$\bar{\alpha}$	apparent change in the angle of attack due to motion
α	mean angle of attack
α_o	amplitude of the unsteady part of the angle of attack
γ	half apex angle of the wedge in Part II
ζ	complex variable in transformed plane
ξ, η	coordinates in ζ - plane
λ	amplitude of the heaving of the plate
ρ	fluid density
σ	choked cavitation number in Part I; also a cavitation number in Part II
φ	acceleration potential
ψ	harmonic conjugate of acceleration potential
ω	oscillatory angular velocity

Subscripts:

c	cavity conditions
s	steady solutions
∞	conditions at upstream infinity

Superscripts:

\sim	amplitude of unsteady part
+ , -	evaluation of functions at $\eta = \pm 0$

General Introduction

The importance of the problem of unsteady cavity flow has become well recognized because of the present day interest in the high speed performance of hydrofoil crafts, ship propellers, pumps and turbines that frequently operate under cavitating conditions. In the case of axial-flow turbomachines, for instance, a possible separation of the flow at the inlet side of the blades may result in the attainment of the vapor pressure with a cavity forming behind the detachment point. It is well known from experiments (References 1, 2, Part II) that when the length of the cavity is somewhat shorter than the chord length of the cavitating hydrofoil, the flow becomes unstable and the cavitating region grows and collapses rather violently, causing noise and severe vibrations to the hydrofoil. On the other hand, when the cavities are much longer, the so-called super-cavitating state, the flow is steady in the mean. In certain cases, the ship propellers and the turbopump impellers may be designed specifically for supercavitating operation condition in order to avoid unstable regions and attendant cavitation damage.

Forces, moments and other performance indices are correspondingly altered in the presence of cavity which in turn requires modification of the design parameters of the machines.

In studying the cavitation phenomenon concerned with individual components such as a hydrofoil or strut, isolated hydrofoils are usually used. On the other hand, a cascade of hydrofoils serves for the purpose of simulating the flow through a cavitating machine, with an obvious advantage of achieving simplicity and an easy access to analysis without

losing essential features of the flow in a complete machine. This type of cascade analysis finds application in design of pumps or propellers of hydrofoil boats. Compared with the steady cascade flow, only little theoretical work has been done on the unsteady cascade flow (see, for example, Reference 10, Part II) and this field has yet to be developed.

Many theoretical approaches (References 6, 7, 8, 9, Part II) have been attempted on the two-dimensional unsteady cavitating flow in an unbounded medium, although at the present time no single theory has been convincingly established because of some inherent difficulties involved in the problem. These difficulties will be briefly mentioned here, and later more about them will be discussed in Part II of the thesis in connection with some representative theories:

One of them is the non-linear boundary condition along the cavity boundary which is not known a priori. Unlike the case of steady cavity flows, the unsteady cavity surface of constant pressure is no longer a surface of constant speed, nor is it a stream surface, but it is a material surface. Hence, the hodograph methods that are so powerful in non-linear theories for steady cavity flow are not applicable in general.

Another fundamental difficulty arises from the behavior of the static pressure at infinity as the cavity volume changes in time. A growing cavity in unbounded flow necessitates a sink at infinity to accommodate the displaced liquid which in turn generates a logarithmically singular pressure at infinity. This singular behavior of the pressure at infinity becomes even more pronounced in internal flow problems. For example, a fluctuating source in the middle of a two-dimensional tunnel can be shown to create a linearly singular pressure at infinity.

In contrast with the above two-dimensional case, however, a singular pressure will never occur in an unbounded three-dimensional flow and thus it may be argued on this ground that the above difficulty is somewhat artificial because any real flow is always finite and also never two-dimensional in the large. In accordance with this point of view, T. B. Benjamin (Reference 14, Part II) first demonstrated the approximate equivalence between the hypothetical plane flow and the inner region of some real three-dimensional flow with small spanwise variations by matching the two-dimensional potentials to the three-dimensional ones, thus eliminating the singularity of the pressure at infinity.

The simplest case of the two-dimensional unsteady cavity flow in infinite fluid is when the cavity extends indefinitely, and this case has been treated by several authors (References 1, 10, Part I; Reference 11, Part II). In this case, because of the absence of the cavity volume fluctuation in time, the question of the singular pressure at infinity does not arise and the analysis becomes simpler accordingly.

The above discussion pertains to unbounded flow problems. An entirely different class of problems occurs in internal flows. These may be typified by flows through water tunnels, hydraulic pumping circuits, etc. One can imagine these systems operating with cavitating components such as hydrofoils and struts, or with sections of cascades representing pumps. Often these internal flows are utilized in water tunnels or wind tunnels to measure the behavior of individual hydrofoils or other devices for the purpose of tests or research on flow phenomena. It may happen that the tunnel boundaries are then not remote from the test object and an unwanted "interference" may occur. This is sometimes

referred to as "wall effect" and it is a common worry to experimenters in both wind and water tunnels in interpreting and correlating the experimental results. Therefore it is not surprising that a relatively large literature has developed both from an aeronautical and a hydrodynamic interest to determine the various wall effects that can arise in experimental situations. Both steady and unsteady cases have been treated in wind tunnel work. But it is only recently that the steady wall effect has been treated in detail for supercavitating flows (References 2, 6, 7, 8, 9, Part I).

Beyond this question of wall effect, an internal flow may be a part of an extensive hydraulic circuit. Thus conditions up- and downstream of a cavitating object in a tube may have quite different unsteady pressures and velocities — unlike the unbounded flow in which velocity fluctuations die off far away.

None of these kinds of problems have been treated yet, and the purpose of the present thesis is to facilitate understanding of the basic pertinent aspects of the cavitating internal flows by considering some simplified situations.

The first part of this thesis is devoted to the study of the wall effect on the unsteady performance coefficients when the cavity length is infinite. This case corresponds to the situation widely known as choked or blocked flow, determination of which is often an important part of water tunnel testing. In our problem, the harmonic motion of a cavitating flat plate will be assumed to create all the possible unsteady disturbances. The cavity pressure is assumed to be constant for all time. The velocity at upstream infinity is assumed to be constant so that no overall mass oscillation is present. Since the length of the cavity is

infinite, the question of the cavity volume change in time does not arise and consequently the pressure disturbance far upstream is assumed to be bounded, but not necessarily zero and it will be determined from the solution itself.

Clearly, the choked cavity is only an idealized limiting case of cavity flow. Nonetheless, this relatively simple situation more easily allows us to extract the information about salient features of the physical phenomenon. Part I of the thesis presented herein appeared in the author's previous publication (Reference 16, Part I).

In Part II of this thesis, we study mass fluctuations in an internal flow containing a cavity. As a representative problem of this type, we consider an unsteady cavity with finite length in a two-dimensional tunnel. The motivation of this study is to understand unsteady characteristics of a hydraulic system in which a cavitating component may participate.

In previous analyses of such unsteady motions (References 12 and 13, Part II), the pressure of the cavity is accounted for by treating it essentially as a "passive compliance". That is, the cavity is assumed to act as a pressurized reservoir and its volume is determined by the local pressure on a steady state basis. This type of approach provides for a change in fluid volume within a given system with pressure and thereby permits the mass oscillations which are known to take place in some turbopump applications. This kind of analysis based on quasi-steady approximation, in which the behavior of the system during the unsteady motion is assumed to be a succession of steady states, is probably all right for very low frequencies of oscillation. But, it is virtually certain that the motion of the cavity surface — as well as the

volume of the cavity itself — is dynamically controlled. It is hoped that the present work may provide a basis of analysis of this general type of flow and show when such quasi-steady models are useful.

The unsteady cavity problems are very difficult to deal with for the reasons mentioned earlier. To make some progress without resorting to a full numerical analysis of the basic governing equations, we will make the essential assumption in both of the problems that the unsteady motion is a small perturbation around some mean steady motion. Further, the cavity-body will be assumed to be slender to avoid tedious mathematics by applying simple linearization techniques.

PART I

THE WALL EFFECT FOR UNSTEADY,
CHOKED SUPERCAVITATING FLOW

1. Introduction

The investigation of the unsteady flow with a cavity forming behind a solid body has recently been the object of great interest. A pioneering work has been done by B. R. Parkin⁽¹⁾ about fully cavitating hydrofoils in an unbounded medium. His later report⁽²⁾ contains some unsteady wedge problems solved by T. Y. Wu. The problem of a supercavitating flat plate in non-uniform motion under a free surface has been studied by C. C. Hsu⁽³⁾. Also C. S. Song⁽⁴⁾ treated the problem of the supercavitating hydrofoil oscillating under the free surface, and later extended his analysis⁽⁵⁾ to a supercavitating flat plate with an oscillating flap.

All these works, however, do not treat the case of an unsteady cavity flow constrained in a channel, which is of considerable practical importance in pumps and turbomachines. In fact, to the author's knowledge no paper has been seen in print on a theoretical investigation about non-steady cavitating flows with the wall boundary effect.

The effect of rigid tunnel walls has been investigated only for steady flows, for instance, by Cohen, Sutherland and Tu⁽⁶⁾, and Fabula⁽⁷⁾, based on linearized theories. Non-linear theories have been developed by Ai and Harrison⁽⁸⁾, and Wu, Whitney and Lin⁽⁹⁾. Geurst⁽¹⁰⁾ treated a partially cavitating hydrofoil in a channel using the mixed analytic function theory on a multiply-connected region.

When both the wall effect and the unsteadiness are to be taken into account, the problem naturally becomes quite complicated so that only the rough assumptions leading to a linearization should seem to prove the problem tractable.

The purpose of this paper is to give a linearized estimate of the wall effect on a supercavitating two-dimensional hydrofoil with harmonic heaving and pitching between infinite parallel walls. Attention will be confined to the case of blocked or choked cavity flow. This so-called choked flow has been treated for a steady case in Reference [2].

The wall effect on the pressure at the upstream infinity is also investigated as an inherent physical nature of the problem.

The analysis presented herein should be of some value to those who study the cavitating phenomena occurring in fluid machinery and to the users of water tunnels.

Although the complexity of the actual physical phenomena might reduce the validity of any linear theory, the simplicity of the theory should override exhausting mathematical difficulties, enabling an easier analysis.

It is hoped that the present theory may provide a stepping stone for study of the wall effect on other more complicated unsteady flows such as unchoked cavity flow, flow past hydrofoils with arbitrary profiles, and most of all, unsteady cavitating cascades.

2. Formulation of the Problem

Consider a flat plate heaving and pitching with small amplitudes in an otherwise uniform two-dimensional incompressible inviscid flow constrained between two infinite parallel walls, as depicted in Fig. 1. We assume a cavity springs from the leading and the trailing edges of the foil and extends to infinity so that a choked flow is established. The pressure on the cavity surface will be assumed to maintain a given constant value for all time.

At this moment no restriction will be imposed on the pressure at the upstream infinity. The cavity-foil will be assumed to form a thin sheet for the purpose of linearization.

The origin of the coordinate system is taken at the mean position of the leading edge of the foil, with the x-axis parallel to the walls and the y-axis orthogonal to them. All dimensions are normalized by the chord length of the hydrofoil.

Let $\vec{q} = U(1+u, v)$ be the velocity vector, where U is the oncoming upstream velocity, u and v are the perturbation velocity components in the x- and the y-direction respectively. The Euler's equation linearized in the perturbation quantities becomes

$$\vec{a} = \left(\frac{\partial}{\partial t} + U \frac{\partial}{\partial x} \right) \vec{q} = -\frac{1}{\rho} \nabla P \quad (1)$$

where $\vec{a} = (a_x, a_y)$ is the acceleration vector, P is the pressure, and ρ is the fluid density.

Now define

$$\nabla \varphi = \frac{1}{U^2} \vec{a} = -\frac{1}{\rho U^2} \nabla P \quad (2)$$

Setting $\varphi = 0$ on the cavity allows one to write

$$\varphi = \frac{P_c - P}{\rho U^2} \quad (3)$$

where P_c is the cavity pressure. φ is called the acceleration potential.

Equation (1) and the continuity equation $\nabla \cdot \vec{q} = 0$ gives

$$\nabla^2 \varphi = 0 \quad (4)$$

It immediately follows that the harmonic conjugate function $\psi(x, y, t)$ of the acceleration potential can be defined by the Cauchy-Riemann relation:

$$\frac{a_x}{U^2} = \frac{\partial \varphi}{\partial x} = \frac{\partial \psi}{\partial y} \quad (5)$$

$$\frac{a_y}{U^2} = \frac{\partial \varphi}{\partial y} = -\frac{\partial \psi}{\partial x}$$

That is, the complex acceleration potential $F(z, t) = \varphi(x, y, t) + i\psi(x, y, t)$ is an analytic function of $z = x + iy$ at every instant of time t . Here i is the unit imaginary number with respect to space.

Now suppose the motion of the hydrofoil is given as in Fig. 2. Then the linearized boundary conditions become

$$\psi(x, 0^-, t) = \psi_m(x, t) \quad 0 < x < 1 \quad (6. a)$$

$$\varphi(x, 0^-, t) = 0 \quad 1 < x < \infty \quad (6. b)$$

$$\varphi(x, 0^+, t) = 0 \quad 0 < x < \infty \quad (6. c)$$

$$\psi(x, -h_2, t) = \psi_\ell(x, t) \quad -\infty < x < \infty \quad (6. d)$$

$$\psi(x, h_1, t) = \psi_u(x, t) \quad -\infty < x < \infty \quad (6. e)$$

where ψ_ℓ , ψ_u , ψ_m are to be determined in such a way as to match the conditions on the walls and at infinity. The boundary conditions are described in Fig. 3.

From Fig. 2, the ordinate of the foil is found

$$Y(x, t) = \lambda e^{j\omega t} - x(\alpha + \alpha_0 e^{j\omega t}) \quad (7)$$

where j is the unit imaginary number with regard to time and α_0 is a complex constant. In what follows, it is understood that only the real part is to be taken unless otherwise indicated. On the hydrofoil, linearization gives rise to

$$Uv = \frac{\partial Y}{\partial t} + U \frac{\partial Y}{\partial x} \quad (8)$$

Thus along the wetted surface of the plate,

$$a_y = \frac{D(Uv)}{Dt} = \frac{\partial^2 Y}{\partial t^2} + 2U \frac{\partial^2 Y}{\partial t \partial x} + U^2 \frac{\partial^2 Y}{\partial x^2}$$

It immediately follows from Equation (5) and the above that

$$-\frac{\partial \psi}{\partial x} = \frac{1}{U^2} \frac{\partial^2 Y}{\partial t^2} + \frac{2}{U} \frac{\partial^2 Y}{\partial t \partial x} + \frac{\partial^2 Y}{\partial x^2} \quad (9)$$

Equation (9) can be integrated to give

$$\psi_m(x, t) = -\frac{1}{U^2} \int_0^x \frac{\partial^2 Y}{\partial t^2} dx - \frac{2}{U} \frac{\partial Y}{\partial t} - \frac{\partial Y}{\partial x} + \psi'_m(t)$$

$\psi'_m(t)$ being a function of time only.

Using Equation (7) in the above equation results in

$$\psi_m(x, t) = \alpha + \left[\alpha_o - 2jk(\lambda - \alpha_o x) + k^2 x \left(\lambda - \frac{\alpha_o}{2} x \right) \right] e^{j\omega t} + \psi'_m(t) \quad (10)$$

in which $k = \omega/U$ is reduced frequency. It seems most appropriate to write $\psi'_m(t) = B_m e^{j\omega t} + \text{constant}$, assuming that the harmonic motion does not cause instability of the flow and that the oscillations occur only at frequency ω . B_m is a constant. Now it is possible to write

$$\psi_m(x, t) = A_m + [B_m + Q(x)] e^{j\omega t} \quad (11)$$

where

$$Q(x) = \alpha_o - 2jk(\lambda - \alpha_o x) + k^2 x \left(\lambda - \frac{\alpha_o}{2} x \right) \quad (12)$$

Here A_m is a constant.

On the upper wall, Equation (9) is also applicable with $Y = h_1$ so that one can write

$$\psi_u(x, t) = A_u + B_u e^{j\omega t} \quad (13)$$

Similarly, on the lower wall,

$$\psi_{\ell}(x, t) = A_{\ell} + B_{\ell} e^{j\omega t} \quad (14)$$

A_u , B_u , A_{ℓ} , and B_{ℓ} are constants.

Now as $x \rightarrow -\infty$, we must have $\psi_u = \psi_{\ell}$. Therefore from Equations (13) and (14), one can set

$$A_u = A_{\ell} = A_w, \quad B_u = B_{\ell} = B_w \quad (15)$$

A Schwarz-Christoffel transformation⁽⁵⁾ given by

$$z = \frac{h_1}{\pi} \log \frac{c_1}{c_1 - \zeta} - \frac{h_2}{\pi} \log \frac{h_2 c_1 + h_1 \zeta}{h_2 c_1} \quad (16)$$

maps the whole flow field in the z -plane into the upper half of the ζ -plane, with the boundaries lying on the real axis of the ζ -plane.

Here c_1 is the root of

$$1 = \frac{h_1}{\pi} \log \frac{c_1}{c_1 + 1} - \frac{h_2}{\pi} \log \frac{h_2 c_1 - h_1}{h_2 c_1} \quad (17)$$

and

$$c_2 = -\frac{h_2}{h_1} c_1$$

The boundary conditions in the ζ -plane are illustrated in Fig. 4.

3. Solution of the Boundary Value Problem

Now define

$$\begin{aligned} F_o(\zeta, t) &= \varphi_o(\xi, \eta, t) + i\psi_o(\xi, \eta, t) \\ &= F(z(\zeta), t) - i(A_w + B_w e^{j\omega t}) \end{aligned} \quad (18)$$

Then the boundary conditions for $F_o(\zeta, t)$ become, in view of Equations (6), (11), (13), (14), (15) and (18),

$$\psi_o(\xi, 0, t) = 0 \quad \xi < c_2 \quad (19. a)$$

$$\varphi_0(\xi, 0, t) = 0 \quad c_2 < \xi < -1 \quad (19. b)$$

$$\psi_0(\xi, 0, t) \equiv \Psi_0(\xi, t) = A_m - A_w + [B_m - B_w + Q(x(\xi))] e^{j\omega t} \quad -1 < \xi < 0 \quad (19. c)$$

$$\varphi_0(\xi, 0, t) = 0 \quad 0 < \xi < c_1 \quad (19. d)$$

$$\psi_0(\xi, 0, t) = 0 \quad \xi > c_1 \quad (19. e)$$

This is a mixed boundary value problem with the real and the imaginary part of the analytic function F_0 alternately given on the whole real axis at every instant of time.

An analytic continuation of F_0 into the lower half of the ζ -plane by defining $F_0(\bar{\zeta}, t) = -\overline{F_0(\zeta, t)}$ brings about the following modified boundary values.

$$F_0^+ + F_0^- = 0 \quad \xi < c_2 \quad (20. a)$$

$$F_0^+ - F_0^- = 0 \quad c_2 < \xi < -1 \quad (20. b)$$

$$F_0^+ + F_0^- = 2i\Psi_0 = 2i\{A_m - A_w + [B_m - B_w + Q(x(\xi))] e^{j\omega t}\} \quad -1 < \xi < 0 \quad (20. c)$$

$$F_0^+ - F_0^- = 0 \quad 0 < \xi < c_1 \quad (20. d)$$

$$F_0^+ + F_0^- = 0 \quad c_1 < \xi \quad (20. e)$$

in which the superscripts refer to the value of F_0 as $\eta \rightarrow \pm 0$. The above is a Hilbert problem the solution of which can be obtained by following the method given in Reference [11].

First consider the homogeneous problem

$$H^+ + H^- = 0 \quad \xi < c_2 \quad (21. a)$$

$$H^+ - H^- = 0 \quad c_2 < \xi < -1 \quad (21. b)$$

$$H^+ + H^- = 0 \quad -1 < \xi < 0 \quad (21. c)$$

$$H^+ - H^- = 0 \quad 0 < \xi < c_1 \quad (21. d)$$

$$H^+ + H^- = 0 \quad c_1 < \xi \quad (21. e)$$

The following requirements will be imposed on the solution:

Condition 1: In the physical plane, the leading edge of the foil should manifest the well-known $1/4$ - singularity. For this discussion, see for example, Reference [10]. Although the argument given therein regards the steady case using the complex velocity, the same should be applicable to the complex acceleration potential because it can be easily shown that the complex acceleration potential is equivalent to the complex velocity potential in the case of steady flow⁽²⁾. The local mapping being $z \sim \zeta^2$ near the origin, this condition in the z -plane corresponds to the $1/2$ - singularity in the ζ -plane; that is, H should behave like $\zeta^{-1/2}$ as $\zeta \rightarrow 0$.

Condition 2: The Kutta condition should be satisfied at the trailing edge.

The general solution to the homogeneous problem is then found to be

$$H(\zeta) = P(\zeta) \cdot \sqrt{\frac{(\zeta+1)(\zeta-c_1)(\zeta-c_2)}{\zeta}} \quad (22)$$

where the branch cuts are to be taken along the real axis $\xi < c_2$, $-1 < \xi < 0$ and $\xi > c_1$, and $P(\zeta)$ is a rational function with real coefficients. Also $P(\zeta)$ should not have any poles in the finite part of the ζ -plane because the only singularity is at the leading edge and the Condition 1 is already taken care of by the square root part of the solution.

Now consider a new function $G(\zeta)$ defined by the relation

$$G(\zeta) = \frac{F_o(\zeta)}{H(\zeta)} \quad (23)$$

From Equations (20) and (21), it follows that

$$G^+ - G^- = \frac{F_o^+}{H^+} - \frac{F_o^-}{H^-} = 0 \quad \xi < c_2 \quad (24.a)$$

$$G^+ - G^- = \frac{F_o^+}{H^+} - \frac{F_o^-}{H^-} = 0 \quad c_1 < \xi < -1 \quad (24. b)$$

$$G^+ - G^- = \frac{F_o^+}{H^+} - \frac{F_o^-}{H^-} = \frac{2i\Psi_o}{P(\xi)} \cdot g(\xi) \quad -1 < \xi < 0 \quad (24. c)$$

$$G^+ - G^- = \frac{F_o^+}{H^+} - \frac{F_o^-}{H^-} = 0 \quad 0 < \xi < c_1 \quad (24. d)$$

$$G^+ - G^- = \frac{F_o^+}{H^+} - \frac{F_o^-}{H^-} = 0 \quad \xi > c_1 \quad (24. e)$$

where

$$g(\xi) = \sqrt{\frac{\xi}{(\xi+1)(\xi-c_1)(\xi-c_2)}} \quad (25)$$

By using Plemelj's formula⁽¹¹⁾, an analytic function in the upper half plane can be expressed, given its values along the entire real axis, according to the equation

$$G(\zeta) = \frac{1}{2\pi i} \int_{-\infty}^{\infty} \frac{G_o(\xi)}{\xi - \zeta} d\xi$$

where

$$G_o(\xi) = G^+(\xi) - G^-(\xi)$$

Now, from Equation (24) and the above two relations, the following equation is immediately obtained.

$$G(\zeta) = \frac{1}{2\pi i} \int_{-1}^0 \frac{2i\Psi_o}{P(\xi)} \frac{g(\xi)}{\xi - \zeta} d\xi \quad (26)$$

Equations (18), (23), (26) and (19. c) finally result in

$$F(z(\zeta), t) = \frac{1}{\pi} \frac{P(\zeta)}{g(\zeta)} \int_{-1}^0 \frac{g(\xi)}{P(\xi)} \cdot \frac{A_m^- A_w^+ [B_m^- B_w^+ Q(x(\xi))] e^{j\omega t}}{\xi - \zeta} d\xi + i (A_w^+ B_w e^{j\omega t})$$

This is the particular solution for the complex acceleration potential. The most general solution to the problem can be obtained by adding to the above a complimentary solution $R(\zeta)/g(\zeta)$, $R(\zeta)$ being a rational function which meets the same requirements as for $P(\zeta)$. Accordingly,

$$F(z(\zeta), t) = \frac{1}{\pi} \frac{P(\zeta)}{g(\zeta)} \int_{-1}^0 \frac{g(\xi)}{P(\xi)} \frac{A_m - A_w + [B_m - B_w + Q(x(\xi))] e^{j\omega t}}{\xi - \zeta} d\xi + i(A_w + B_w e^{j\omega t}) + \frac{R(\zeta)}{g(\zeta)} \quad (27)$$

Now $P(\zeta)$ and $R(\zeta)$ should be so determined as to satisfy the following requirements:

- (i) As $|\zeta| \rightarrow \infty$, $|F(\zeta, t)|$ should be bounded and non-zero. This is the pressure condition at infinity.
- (ii) The only singularity occurs at the leading edge of the foil.
- (iii) This singularity should exhibit the recognized behavior of $1/4$ -singularity in the physical plane, namely, it should behave like $\zeta^{-1/2}$ near the origin in the ζ -plane.
- (iv) The solution should be regular at the trailing edge of the plate.

The immediate consequence of the above conditions is that we must have $P(\zeta) = \text{constant}$ and $R(\zeta) \equiv 0$. Equation (27) now simplifies to

$$F(z(\zeta), t) = \frac{1}{\pi} \frac{1}{g(\zeta)} \int_{-1}^0 \frac{g(\xi) \{A_m - A_w + [B_m - B_w + Q(x(\xi))] e^{j\omega t}\}}{\xi - \zeta} d\xi + i(A_w + B_w e^{j\omega t}) \quad (28)$$

We now proceed to determine $A_m - A_w$ and $B_m - B_w$. Adopting the subscript s for steady limit, we are allowed to write from Equation (28)

$$F_s(\zeta) = \frac{1}{\pi g(\zeta)} \int_{-1}^0 \frac{g(\xi)(A_m - A_w)}{\xi - \zeta} d\xi + iA_w \quad (29)$$

Thus as $z \rightarrow -\infty$, i. e., as $|\zeta| \rightarrow \infty$,

$$F_s(x=-\infty) = -\frac{1}{\pi} \int_{-1}^0 g(\xi)(A_m - A_w) d\xi + iA_w$$

or

$$\varphi_s(x=-\infty) = -\frac{1}{\pi}(A_m - A_w) \int_{-1}^0 g(\xi) d\xi \quad (30)$$

But

$$\varphi_s(x=-\infty) = \frac{P_c - P_s \infty}{\rho U^2} = -\frac{1}{2} \sigma \quad (31)$$

where σ is the cavity number defined by

$$\sigma = \frac{P_s \infty - P_c}{\frac{1}{2} \rho U^2}$$

Equations (30) and (31) give

$$A_m - A_w = \frac{\pi}{2I} \sigma \quad (32)$$

where

$$I = \int_{-1}^0 g(\xi) d\xi$$

It is now necessary to find the choked cavity number. For this purpose let us introduce the complex perturbation velocity $W(z) = u - iv$ for the steady flow. Using the linearized Bernoulli equation, one obtains the following boundary conditions:

$$v = 0 \text{ on the two walls}$$

$$u = \sqrt{1 + \sigma} - 1 \text{ on the cavity}$$

$$v = -\alpha \sqrt{1 + \sigma} \text{ on the wetted surface of the foil}$$

The detailed derivation of the above boundary conditions is given in Reference [2]. Let

$$W_o(\zeta) = W(z(\zeta)) - (\sqrt{1+\sigma} - 1) = u_o - iv_o \quad (33)$$

Then in the ζ -plane,

$$\begin{aligned} v_o &= 0 & \xi < c_2 \\ u_o &= 0 & c_2 < \xi < -1 \\ v_o &= -\alpha\sqrt{1+\sigma} & -1 < \xi < 0 \\ u_o &= 0 & 0 < \xi < c_1 \\ v_o &= 0 & \xi > c_1 \end{aligned}$$

Following the same procedure as was employed in obtaining Equation (28), one arrives at

$$W_o(\zeta) = \frac{1}{\pi g(\zeta)} \int_{-1}^0 g(\xi) \frac{\alpha\sqrt{1+\sigma}}{\xi-\zeta} d\xi \quad (34)$$

Equations (33) and (34) imply

$$W(z(\zeta)) = \frac{1}{\pi g(\zeta)} \int_{-1}^0 g(\xi) \frac{\alpha\sqrt{1+\sigma}}{\xi-\zeta} d\xi + \sqrt{1+\sigma} - 1 \quad (35)$$

The solution in Equation (35) is seen to satisfy the Conditions (ii) ~ (iv).

The Condition (i) should now read $W(|\zeta| = \infty) = 0$ since $u = v = 0$ at $z = -\infty$.

Consequently, Equation (35) gives

$$\sigma = \frac{1}{\left(1 - \frac{\alpha}{\pi} I\right)^2} - 1 \quad (36)$$

Equations (32) and (36) result in

$$A_m - A_w = \frac{\pi}{2I} \left[\frac{1}{\left(1 - \frac{\alpha}{\pi} I\right)^2} - 1 \right] \quad (37)$$

Table 1 shows the choked cavity numbers σ calculated from Equation (36) for the case of $h_1 = h_2$ at various angles of attack α .

Values of $\frac{\sigma}{\alpha}$ for $\alpha \rightarrow 0$ as function of the tunnel height given by Parkin⁽²⁾ and Fabula⁽⁷⁾ can be easily shown to coincide with those given by Equation (36). Also comparison of the results in Table 1 with those of Cohen, Sutherland and Tu⁽⁶⁾ gives a good agreement. A slight deviation from the result of Cohen et al for large α 's is probably due to the different boundary conditions used on the cavity. Namely, the present theory employs $u = \sqrt{1 + \sigma} - 1$ on the cavity, whereas their result is based on $u = \frac{1}{2}\sigma$ on the cavity.

In order to determine $B_m - B_w$, assume

$$\psi(x, y, t) = \psi_s(x, y) + \tilde{\psi}(x, y)e^{j\omega t} \quad (38. a)$$

$$v(x, y, t) = v_s(x, y) + \tilde{v}(x, y)e^{j\omega t} \quad (38. b)$$

where the subscript s denotes the steady solutions.

For the steady limit, Equations (1) and (5) enable us to write

$$-\frac{\partial \psi_s}{\partial x} = \frac{\partial v_s}{\partial x}$$

Equations (1), (5) and (38) together with the above relation give the equation

$$jk\tilde{v} + \frac{\partial \tilde{v}}{\partial x} = -\frac{\partial \tilde{\psi}}{\partial x}$$

which has the integral, along the real axis,

$$\tilde{v}(x, 0) = -e^{-jkx} \int_{-\infty}^x \frac{\partial \tilde{\psi}(x', 0)}{\partial x'} e^{jkx'} dx', \quad (39)$$

the condition that $v = 0$ at $x = -\infty$ having been incorporated. The integral depends only on the end points and is independent of the path of integration. Integrating Equation (39) by parts and evaluating at $(0^+, 0^-)$, one obtains

$$\tilde{v}(0^+, 0^-) = - \left\{ \tilde{\psi}(x, 0^-) e^{jkx} \Big|_{-\infty}^{0^+} - jk \int_{-\infty}^0 \tilde{\psi}(x, 0^-) e^{jkx} dx \right\}. \quad (40)$$

It is most convenient to carry out the integration along the η -axis in the

ζ -plane. Set $F(z(\zeta), t) = F_s(\zeta) + \tilde{F}(\zeta)e^{j\omega t}$ in Equation (28) to obtain

$$\tilde{F}(\zeta) = \frac{1}{\pi g(\zeta)} \int_{-1}^0 g(\xi) \frac{B_m - B_w + Q(x(\xi))}{\xi - \zeta} d\xi + iB_w$$

Then along the η -axis

$$\text{Im } \tilde{F}(i\eta) = B_w + (B_m - B_w) \text{Im } \tilde{F}_a(i\eta) + \text{Im } \tilde{F}_b(i\eta) \quad (41)$$

where

$$\tilde{F}_a(i\eta) = \frac{1}{\pi g(i\eta)} \int_{-1}^0 \frac{g(\xi)}{\xi - i\eta} d\xi \quad (42. a)$$

$$\tilde{F}_b(i\eta) = \frac{1}{\pi g(i\eta)} \int_{-1}^0 \frac{g(\xi) \cdot Q(x(\xi))}{\xi - i\eta} d\xi \quad (42. b)$$

From Equations (7) and (8) is obtained

$$\tilde{v}(0^+, 0^-) = j\lambda k - \alpha_o \quad (43)$$

Also from Equations (11), (12), (13) and (15) follow

$$\tilde{\psi}(0^+, 0^-) = B_m + \alpha_o - 2jk\lambda \quad (44. a)$$

$$\tilde{\psi}(-\infty, 0^-) = B_w \quad (44. b)$$

Combining Equations (43), (44) and (40), one can write

$$j\lambda k - \alpha_o = -\left\{ B_m + \alpha_o - 2jk\lambda - B_w e^{jkx} \Big|_{x=-\infty} - jk \int_{-\infty}^0 \text{Im } \tilde{F}(i\eta) e^{jkx} dx \right\} \quad (45)$$

From Equations (45), (41) and (42) is obtained

$$jk\lambda = (B_m - B_w)(1 - jkJ_a) - jkJ_b$$

in which

$$J_a = \int_{-\infty}^0 \text{Im } \tilde{F}_a(i\eta) e^{jkx} dx$$

and
$$J_b = \int_{-\infty}^0 \text{Im } \tilde{F}_b(i\eta) e^{jkx} dx .$$

This finally gives

$$B_m - B_w = jk \frac{\lambda + J_b}{1 - jk J_a} \quad (46)$$

Equation (42. a) can be written

$$\tilde{F}_a(i\eta) = \frac{1}{\pi} \left(\sqrt{a^2 + b^2} e^{i\theta} \right)^{1/2} \int_{-1}^0 g(\xi) \frac{\xi + i\eta}{\xi^2 + \eta^2} d\xi \quad (47)$$

with

$$a = -(\eta^2 + c_1 + c_2 - c_1 c_2) \quad (48.a)$$

$$b = -\frac{\eta^2(c_1 + c_2 - 1) + c_1 c_2}{\eta} \quad (48.b)$$

$$\theta = \tan^{-1} \frac{b}{a} \quad (48.c)$$

Since $\eta > 0$, we need $\pi/2 < \theta < \pi$ by comparing Equation (42.a) with Equation (47) and considering the branch cuts for $g(i\eta)$ so that we must have

$$\cos \frac{\theta}{2} , \quad \sin \frac{\theta}{2} > 0 \quad (49)$$

Set $r = \sqrt{a^2 + b^2}$ and use Equation (48) to get

$$\sin \frac{\theta}{2} = \left(\frac{r-a}{2r} \right)^{1/2} , \quad \cos \frac{\theta}{2} = \left(\frac{r+a}{2r} \right)^{1/2}$$

These are seen to satisfy the condition (49).

Combining Equations (47) and (48) gives rise to

$$\text{Im } \tilde{F}_a(i\eta) = \frac{1}{\pi} \int_{-1}^0 g(\xi) \frac{\xi \left(\frac{r-a}{2} \right)^{1/2} + \eta \left(\frac{r+a}{2} \right)^{1/2}}{\xi^2 + \eta^2} d\xi \quad (50)$$

Similarly, Equation (42.b) reduces to

$$\text{Im } \hat{F}_b(i\eta) = \frac{1}{\pi} \int_{-1}^0 g(\xi) Q(x(\xi)) \frac{\xi \left(\frac{r-a}{2}\right)^{1/2} + \eta \left(\frac{r+a}{2}\right)^{1/2}}{\xi^2 + \eta^2} d\xi \quad (51)$$

Let us write

$$J_a = J_1 + J_2 \quad , \quad \text{and } J_b = J_3 + J_4$$

where

$$J_1 = \frac{1}{\pi} \int_{-\infty}^0 \left(\frac{r-a}{2}\right)^{1/2} \int_{-1}^0 g(\xi) \frac{\xi d\xi}{\xi^2 + \eta^2} e^{jkx} dx \quad (52)$$

$$J_2 = \frac{1}{\pi} \int_{-\infty}^0 \left(\frac{r+a}{2}\right)^{1/2} \int_{-1}^0 g(\xi) \frac{\eta d\xi}{\xi^2 + \eta^2} e^{jkx} dx \quad (53)$$

$$J_3 = \frac{1}{\pi} \int_{-\infty}^0 \left(\frac{r-a}{2}\right)^{1/2} \int_{-1}^0 g(\xi) Q(x(\xi)) \frac{\xi d\xi}{\xi^2 + \eta^2} e^{jkx} dx \quad (54)$$

$$J_4 = \frac{1}{\pi} \int_{-\infty}^0 \left(\frac{r+a}{2}\right)^{1/2} \int_{-1}^0 g(\xi) Q(x(\xi)) \frac{\eta d\xi}{\xi^2 + \eta^2} e^{jkx} dx \quad (55)$$

Using Equation (12) and incorporating Equation (52), Equation (54) can be written

$$J_3 = (\alpha_o - 2jk\lambda) J_1 + (2jk\alpha_o + k^2\lambda) J_{3a} - \frac{\alpha_o}{2} k^2 J_{3b} \quad (56)$$

where

$$J_{3a} = \frac{1}{\pi} \int_{-\infty}^0 \left(\frac{r-a}{2}\right)^{1/2} \int_{-1}^0 g(\xi) x(\xi) \frac{\xi d\xi}{\xi^2 + \eta^2} e^{jkx} dx \quad (57)$$

and

$$J_{3b} = \frac{1}{\pi} \int_{-\infty}^0 \left(\frac{r-a}{2}\right)^{1/2} \int_{-1}^0 g(\xi) x^2(\xi) \frac{\xi d\xi}{\xi^2 + \eta^2} e^{jkx} dx \quad (58)$$

Similarly,

$$J_4 = (\alpha_o - 2jk\lambda) J_2 + (2jk\alpha_o + k^2\lambda) J_{4a} - \frac{\alpha_o}{2} k^2 J_{4b} \quad (59)$$

where

$$J_{4a} = \frac{1}{\pi} \int_{-\infty}^0 \left(\frac{r+a}{2}\right)^{1/2} \int_{-1}^0 g(\xi)x(\xi) \frac{\eta d\xi}{\xi^2 + \eta} e^{jkx} dx \quad (60)$$

and

$$J_{4b} = \frac{1}{\pi} \int_{-\infty}^0 \left(\frac{r+a}{2}\right)^{1/2} \int_{-1}^0 g(\xi)x^2(\xi) \frac{\eta d\xi}{\xi^2 + \eta} e^{jkx} dx \quad (61)$$

Equation (46) now becomes

$$B_m - B_w = jk \frac{\lambda + J_3 + J_4}{1 - jk(J_1 + J_2)} \quad (62)$$

with J_1 and J_2 given by Equations (52) and (53), and J_3 and J_4 given by Equations (56)~(61). Equations (28), (37) and (62) completely determine the acceleration potential $\varphi(x, y, t)$ for the problem. Discussion on the convergence of the above integrals and the numerical calculation procedure are described in Appendix 1.

4. Pressure at Infinity, Force and Moment

The pressure at the upstream infinity is readily found from the acceleration potential. Taking $|\zeta| \rightarrow \infty$, i. e., $x \rightarrow -\infty$, in Equation (28) gives rise to

$$\varphi(x=-\infty, t) = \frac{P_c - P_{\infty}(t)}{\rho U^2} = -\frac{1}{\pi} \int_{-1}^0 g(\xi) \left\{ A_m - A_w + [B_m - B_w + Q(x(\xi))] e^{j\omega t} \right\} d\xi$$

Let $P_{\infty}(t) = P_{s\infty} + \tilde{P}_{\infty} e^{j\omega t}$, then it follows that

$$\frac{\tilde{P}_{\infty}}{\rho U^2} = \frac{1}{\pi} \int_{-1}^0 g(\xi) [B_m - B_w + Q(x(\xi))] d\xi \quad (63)$$

The force coefficient is defined by

$$C_f = \frac{f}{\frac{1}{2} \rho U^2}$$

Here f is the force exerted on the hydrofoil which is calculated from

$$f = \int_0^1 (P - P_c) dx = \int_{-1}^0 (P_c - P) \frac{dx}{d\xi} d\xi \quad .$$

In terms of the acceleration potential, the force coefficient becomes

$$C_f = 2 \int_{-1}^0 \varphi(x(\xi)) \frac{dx}{d\xi} d\xi \quad (64)$$

Defining the moment coefficient about the leading edge (tail up positive) as

$$C_m = \frac{\int_0^1 (P - P_c) x dx}{\frac{1}{2} \rho U^2}$$

we can write

$$C_m = 2 \int_{-1}^0 \varphi(x(\xi)) x(\xi) \frac{dx}{d\xi} \cdot d\xi \quad (65)$$

In what follows, \oint denotes the Cauchy principle value of the integral. Then

$$\varphi(x(\xi)) = \frac{1}{\pi g(\xi)} \oint_{-1}^0 \left\{ A_m - A_w + [B_m - B_w + Q(x(\tau))] e^{j\omega\tau} \right\} \frac{g(\tau) d\tau}{\tau - \xi}$$

Setting $C_f = C_{fs} + \tilde{C}_f e^{j\omega t}$, where C_{fs} is the steady solution, allows one to obtain the following expression

$$\tilde{C}_f = \frac{2}{\pi} \int_{-1}^0 \frac{1}{g(\xi)} \oint_{-1}^0 [B_m - B_w + Q(x(\tau))] \frac{g(\tau) d\tau}{\tau - \xi} \frac{dx}{d\xi} d\xi \quad (66)$$

Similarly, writing $C_m = C_{ms} + \tilde{C}_m e^{j\omega t}$ gives

$$\tilde{C}_m = \frac{2}{\pi} \int_{-1}^0 \frac{1}{g(\xi)} \oint_{-1}^0 [B_m - B_w + Q(x(\tau))] \frac{g(\tau) d\tau}{\tau - \xi} \cdot x(\xi) \frac{dx}{d\xi} d\xi \quad (67)$$

Convergence and numerical calculation procedure for the integrals in Equations (66) and (67) are discussed in Appendix 2.

Specific Cases :

A. Heaving Motion

In this case, $\alpha_o = 0$. Equation (12) now reduces to

$$Q(x) = -2jk\lambda + k^2\lambda x \quad (68)$$

Also Equation (62) becomes

$$B_m - B_w = jk \frac{\lambda - 2jk\lambda(J_1 + J_2) + k^2\lambda(J_{3a} + J_{4a})}{1 - jk(J_1 + J_2)} \quad (69)$$

From Equation (7), the unsteady part of the heave is found to be

$$\frac{\partial Y}{\partial t} = j\omega\lambda e^{j\omega t}$$

The apparent change in the angle of attack due to heaving is then

$$\bar{\alpha} = \frac{-j\omega\lambda e^{j\omega t}}{U} = -j\lambda k e^{j\omega t}$$

It seems most appropriate to normalize the physical quantities by $\bar{\alpha}$ as follows

$$\frac{|\tilde{P}_\infty e^{j\omega t}|}{\frac{1}{2}\rho U^2 |\bar{\alpha}|} = \frac{|\tilde{P}_\infty|}{\frac{1}{2}\rho U^2 \lambda k} \quad (70)$$

$$\frac{\tilde{C}_f e^{j\omega t}}{\bar{\alpha}} = C_{F_r} + jC_{F_i} \quad (71)$$

$$\frac{\tilde{C}_m e^{j\omega t}}{\bar{\alpha}} = C_{M_r} + jC_{M_i} \quad (72)$$

In the above, $C_{F_r} = -\frac{1}{\lambda k} \text{Im } \tilde{C}_f$ is the normalized force coefficient in phase with the apparent change in the angle of attack, and $C_{F_i} = \frac{1}{\lambda k} \text{Re } \tilde{C}_f$ is the quadrature component. Similarly, $C_{M_r} = -\frac{1}{\lambda k} \text{Im } \tilde{C}_m$ and $C_{M_i} = \frac{1}{\lambda k} \text{Re } \tilde{C}_m$ respectively represent the normalized in-phase and quadrature moment

coefficients with regard to the apparent change in the angle of attack due to heaving.

B. Pitching Motion

For a harmonic pitching motion about the leading edge, $\lambda=0$, and Equation (12) becomes

$$Q(x) = \alpha_o \left(1 + 2jkx - \frac{k^2 x^2}{2} \right) \quad (73)$$

Also Equation (62) now reads

$$B_m - B_w = j\alpha_o k \frac{J_1 + J_2 + 2jk(J_{3a} + J_{4a}) - \frac{1}{2}k^2(J_{3b} + J_{4b})}{1 - jk(J_1 + J_2)} \quad (74)$$

The apparent change in the angle of attack is $\bar{\alpha} = \alpha_o e^{j\omega t}$ and normalization of the physical quantities will be made with respect to $\bar{\alpha}$. That is,

$$\frac{|\tilde{P}_\infty e^{j\omega t}|}{\frac{1}{2}\rho U^2 |\bar{\alpha}|} = \frac{|\tilde{P}_\infty|}{\frac{1}{2}\rho U^2 |\alpha_o|} \quad (75)$$

$$\frac{\tilde{C}_f e^{j\omega t}}{\bar{\alpha}} = C_{F_r} + jC_{F_i} \quad (76)$$

$$\frac{\tilde{C}_m e^{j\omega t}}{\bar{\alpha}} = C_{M_r} + jC_{M_i} \quad (77)$$

where $C_{F_r} = \frac{1}{\alpha_o} \text{Re } \tilde{C}_f$ and $C_{M_r} = \frac{1}{\alpha_o} \text{Re } \tilde{C}_m$ are the normalized force and moment coefficients in phase with the apparent change in the angle of attack due to pitching, and $C_{F_i} = \frac{1}{\alpha_o} \text{Im } \tilde{C}_f$ and $C_{M_i} = \frac{1}{\alpha_o} \text{Im } \tilde{C}_m$ are the quadrature components of the normalized force and the moment coefficient respectively.

5. Formulation of an Equivalent Problem

An equivalent problem can be formulated in which the pressure at the upstream infinity is maintained constant at the expense of the steadiness

of the cavity pressure. Suppose we have the same flow as before except that this time we impose the pressure at the upstream infinity to be constant, i. e. $P_{\infty} \equiv P_{s \infty}$. Let the cavity pressure be

$$P_c(t) = P_{cs} + \tilde{P}_c e^{j\omega t} \quad (78)$$

and define the acceleration potential for the new problem as

$$\varphi = \frac{P_c(t) - P}{\rho U^2} \quad (79)$$

It is easy to see that the same boundary conditions as were used in Equation (6) are established for this new problem and following precisely the same procedure will lead us to the same solution. Therefore, we have only to determine \tilde{P}_c in such a way as to make the pressure at the upstream infinity constant. Now, at the upstream infinity, i. e., as $|\zeta| \rightarrow \infty$, Equation (28) gives

$$\varphi(x=-\infty) = -\frac{1}{\pi} \int_{-1}^0 g(\xi) \{A_m - A_w + [B_m - B_w + Q(x(\xi))] e^{j\omega t}\} d\xi$$

Also, from Equations (78) and (79),

$$\varphi(x=-\infty) = \frac{P_{cs} + \tilde{P}_c e^{j\omega t} - P_{\infty}}{\rho U^2}$$

Therefore we must have

$$\frac{\tilde{P}_c}{\rho U^2} = -\frac{1}{\pi} \int_{-1}^0 g(\xi) [B_m - B_w + Q(x(\xi))] d\xi \quad (80)$$

Equation (80) compared with Equation (63) implies that we should have

$$\tilde{P}_c = -\tilde{P}_{\infty} \quad (81)$$

where \tilde{P}_{∞} is the amplitude of the fluctuating part of the pressure at the upstream infinity in the previous problem, and \tilde{P}_c is the amplitude of the unsteady part of the cavity pressure in the new problem.

In other words, in order to maintain the pressure at the upstream infinity constant, the cavity pressure has to be modified, and Equation (81) shows that this modified part must just equal the negative of the unsteady part of the upstream pressure for the old problem. The force and the moment coefficients will remain the same as before, and these two problems are equivalent. Of course, an obvious extension of this argument could be made to include unsteadiness in both the pressure at the upstream infinity and the cavity pressure. However, this case does not seem to be of any practical interest, since in most problems either the cavity pressure or the upstream infinity pressure is specified to be constant.

6. Numerical Results and Discussion

The numerical data presented herein are for the case of the hydrofoil situated in the middle of the channel, namely, $h_1 = h_2 = h$. In this case, $c_1 = -c_2 = c$, and the Equation (16) simplifies to

$$z = \frac{h}{\pi} \log \frac{c^2}{c^2 - \zeta^2} \quad (82)$$

Thus along $\eta = 0$,

$$x(\xi) = \frac{h}{\pi} \log \frac{c^2}{c^2 - \xi^2} \quad (83)$$

And along $\xi = 0$,

$$x(\eta) = \frac{h}{\pi} \log \frac{c^2}{c^2 + \eta^2} \quad (84)$$

All the computation has been carried out on IBM 360 digital computer at the Booth Computing Center, California Institute of Technology.

Figure 5 shows the normalized pressure fluctuation at the upstream infinity given by Equations (70) and (75). The fluctuation is seen to die out

as the walls move apart, as might be expected. It increase as the reduced frequency increases. As the reduced frequency approaches zero finite limits are achieved for various channel heights. In this case, Equation (63) by use of Equations (56), (59), (62), and the appropriate expression for $Q(x)$ results in

$$\lim_{k \rightarrow 0} \frac{|\tilde{P}_{\infty}|}{\frac{1}{2} \rho U^2 |\bar{\alpha}|} = \frac{2}{\pi} \int_{-1}^0 g(\xi) d\xi = \frac{2}{\pi} I$$

But Equation (36) gives

$$\lim_{\alpha \rightarrow 0} \frac{\sigma}{\alpha} = \frac{2}{\pi} I$$

Therefore, as $k \rightarrow 0$, the normalized amplitude of the unsteady part of the upstream pressure approaches the steady limit of $\frac{\sigma}{\alpha}$ as $\alpha \rightarrow 0$, the condition in the channel being maintained choked. Comparison of the values of $\frac{\sigma}{\alpha}$ with those of others was already mentioned at the end of Equation (37).

Figure 6(a) and Figure 6(b) present the normalized unsteady force and moment coefficients for heaving oscillation at various reduced frequencies. Parkin's⁽¹³⁾ data for the case of unbounded flow is also plotted. As might have been expected, the presence of the walls has an effect of increasing the coefficients as the wall height decreases. A linear dependence of the quadrature components on the reduced frequency is pronounced. Because of the way these coefficients have been normalized, they have the phase difference of $\frac{\pi}{2}$ from the hydrofoil velocity and so are in phase with the acceleration of the hydrofoil, hence representing the effect of the apparent mass. The in-phase force coefficients for heaving properly converted from Kelly's⁽¹⁵⁾ data for the case of unbounded medium seem to give an agreeable tendency up to reduced frequency of about 1. For example, at $\alpha = 10^\circ$, $C_{F_r} = 1.11$ ($k = 0.0910$), $C_{F_r} = 1.16$ ($k = 0.3636$), $C_{F_r} = 1.269$

($k = 0.8181$). However, for larger reduced frequencies the values of C_{F_r} calculated from Kelley's data show an uncertain irregularity, even decreasing with reduced frequency (e. g., $C_{F_r} = 2.61$ for $k = 5.4546$ and $C_{F_r} = 2.01$ for $k = 8.1818$). This behavior is not observed in either Parkin's or ours and the reason for this is not clear at this moment. The quadrature components obtained from Kelly's report (for $\alpha = 10^\circ$, say) can be shown to lie slightly above Parkin's data and the behavior seems to be consistent and almost linear in reduced frequency as to be expected.

A set of experimental data obtained by DeLong and Acosta⁽¹⁴⁾ is also plotted in Figure 6(a). The experiment was performed for a hydrofoil at the mean angle of attack $\alpha = 8^\circ$ in a choked tunnel with $h_1 = 2$ and $h_2 = 3$. Although there is seen a qualitative agreement in general tendency between the theoretical and the experimental values, the quantitative discrepancy between them seems to be rather severe. For one thing, the experimental data lie even below Parkin's theoretical values for unbounded medium. Among numerous factors that could possibly explain this deviation, the following might be the most important ones:

In developing our theory, the unsteady part was completely separated from the steady part and there was assumed to be no interaction between them at all. Consequently, the unsteady part of the solution was expressed in terms of the unsteady parameters only and nowhere in it was contained the effect of the steady angle of attack α . In real flow, however, we should certainly expect the effect of the mean angle of attack on the unsteady solution, especially when α is not quite small enough. Our assumption should be good only as $\alpha \rightarrow 0$. Next, there is no way of knowing the actual situation in the tunnel during the experiment caused by the effects such as, for instance, "breathing" of the tunnel on account of bending of the walls due to

the pressure fluctuation. Finally, the flow in the experiment was not strictly two-dimensional because of the cavity attached to the supporting strut.

In Figure 7(a) and Figure 7(b) are shown the normalized unsteady force and moment coefficients for pitching oscillation. Again, the quadrature components are seen to vary linearly with the reduced frequency. For sufficiently small and sufficiently large reduced frequencies the magnitude of the in-phase components increases as the walls are brought closer, whereas overlapping occurs for the reduced frequencies lying somewhere in between.

As the reduced frequency approaches zero, finite limits are obtained for both the heaving and the pitching. Using either Equations (68), (69) and (66), or Equations (73), (74) and (66), one obtains

$$\lim_{k \rightarrow 0} \frac{\tilde{C}_f e^{j\omega t}}{\alpha} = \frac{2}{\pi} \int_{-1}^0 \frac{1}{g(\xi)} \oint_{-1}^0 \frac{g(\tau) d\tau}{\tau - \xi} \frac{dx}{d\xi} d\xi$$

Now, the force coefficient for steady flow is

$$C_{fs} = 2 \int_{-1}^0 \varphi_s(x(\xi)) \frac{dx}{d\xi} d\xi$$

But Equations (28) gives

$$\varphi_s(x(\xi)) = \frac{1}{\pi} \frac{1}{g(\xi)} \oint_{-1}^0 \frac{g(\tau) \cdot (A_m - A_w)}{\tau - \xi} d\tau$$

From Equation (37), one finds

$$A_m - A_w = \alpha + O(\alpha^2) \text{ as } \alpha \rightarrow 0$$

The above three equations result in

$$\lim_{\alpha \rightarrow 0} \frac{C_{fs}}{\alpha} = \frac{2}{\pi} \int_{-1}^0 \frac{1}{g(\xi)} \oint_{-1}^0 \frac{g(\tau) d\tau}{\tau - \xi} \frac{dx}{d\xi} d\xi$$

Thus one finally obtains

$$\lim_{k \rightarrow 0} \frac{\tilde{C}_f e^{j\omega t}}{\bar{\alpha}} = \lim_{\alpha \rightarrow 0} \frac{C_{fs}}{\alpha}$$

That is, the normalized force coefficient as $k \rightarrow 0$ reduces to the steady force coefficient normalized with respect to the angle of attack as the angle of attack approaches zero with choked condition maintained in the tunnel.

Although not given here, values of

$$\lim_{k \rightarrow 0} \frac{\tilde{C}_f e^{j\omega t}}{\bar{\alpha}}$$

calculated from the present theory is easily confirmed to be in excellent agreement with values of

$$\lim_{\alpha \rightarrow 0} \frac{C_{fs}}{\alpha}$$

obtained from Fabula's⁽⁷⁾ report. Readers referring to the force coefficient ratio of choked flow to unbounded flow plotted in References 7 and 8 might wonder why this ratio increases as the walls move away whereas our values of

$$\lim_{k \rightarrow 0} \frac{\tilde{C}_f e^{j\omega t}}{\bar{\alpha}}$$

clearly show the opposite tendency. This confusion should be cleared by noting that in the above references the force ratio (choked flow/unbounded flow) is taken at the same $\frac{\sigma}{\bar{\alpha}}$ for both flows.

Similarly, one finds that

$$\lim_{k \rightarrow 0} \frac{\tilde{C}_m e^{j\omega t}}{\bar{\alpha}} = \lim_{\alpha \rightarrow 0} \frac{C_{ms}}{\alpha}$$

where C_{ms} is the moment coefficient for the steady flow, and α is the steady angle of attack.

7. Conclusion

The numbers predicted by the theory are seen to be self-consistent and their general behavior is qualitatively in good agreement with the already established theory for unbounded flow. The theoretical values show the general tendency similar to the one manifested by a set of experimental data although the quantitative comparison between them seems to be somewhat unfitting. Also the limiting values for zero reduced frequency recover the anticipated steady limits that are physically plausible and these numbers agree well with those of known steady theories. It seems that in order to maintain the choked condition we cannot specify both the cavity pressure and the pressure at the upstream infinity to be time independent, but instead at least one of them has to be relaxed.

If the combination of the amplitude and the reduced frequency of the unsteady motion reaches a certain limit, it could possibly happen in a real flow that the cavity detachment may no longer occur at the trailing edge or the leading edge of the plate. An experimental confirmation on this as a test for the range of validity of the linear theory might provide an interesting investigation.

A direct extension of the present theory is possible to account for arbitrary hydrofoil shape as long as the slope and the angle of attack of the hydrofoil are small enough. It is also hoped that the present analysis may be applicable to the study of the unsteady cascade flow problem.

References

1. B.R. Parkin, "Fully Cavitating Hydrofoils in Non-Steady Motion", California Institute of Technology, Engineering Division Report Number 85-2, July 1957.
2. B. R. Parkin, "Linearized Theory of Cavity Flow in Two Dimensions", Rand Corporation Report P-1745, 1959.
3. C.C. Hsu, "Fully Cavitating Hydrofoils in Nonuniform Motion Under a Free Surface", Journal of Ship Research, Vol. 8, No. 4, March 1965.
4. C.S. Song, "Two-Dimensional Supercavitating Plate Oscillating Under a Free Surface", Journal of Ship Research, Vol. 9, No.1, June 1965.
5. C.S. Song, "Supercavitating Flat Plate With an Oscillating Flap at Zero Cavitation Number", Journal of Ship Research, Vol. 11, No. 1, March 1967.
6. H. Cohen, C.D. Sutherland and Y. Tu, "Wall Effects in Cavitating Hydrofoil Flow", Journal of Ship Research, Vol. 1, No.3, Nov. 1957. See also Rensselaer Polytechnic Institute Math Report, No. 6, Oct. 1956, and Math Report, No. 7, April 1957.
7. A.G. Fabula, "Choked Flow About Vented or Cavitating Hydrofoils", Journal of Basic Engineering, Trans. ASME, Series D, Vol. 86, September 1964.
8. D.K. Ai and Z.L. Harrison, "The Wall Effect in Cavity Flow", California Institute of Technology, Hydrodynamics Laboratory Report No. 111.3, April 1965. Also see Journal of Basic Engineering, Trans. ASME, Series D. Vol. 88, March 1966.
9. T.Y. Wu, and A.K. Whitney and see J.D. Lin, "Wall Effects in Cavity Flows", California Institute of Technology, Division of Engineering and Applied Science Report No. E-111A.5, August 1969.
10. J.A. Geurst, Linearized Theory of Two-Dimensional Cavity Flows, Thesis, Delft University of Technology, May 3, 1961.
11. N.I. Muskhelishvili, Singular Integral Equations, P. Noordhoff Ltd., Gronigen, Holland, 1946.
12. Berezin and Zhidkov, Computing Methods, Vol. 1, Addison Wesley, 1965.
13. B.R. Parkin, "Numerical Data on Hydrofoil Response to Nonsteady Motions at Zero Cavitation Number", Journal of Ship Research, Vol. 6 No. 3, December 1962.
14. R.K. DeLong and A.J. Acosta, "Experimental Investigation of Non-Steady Forces on Hydrofoils Oscillating in Heave", California Institute of Technology, Engineering Division Report, March 1969.

15. H. R. Kelly, "An Extension of the Woods Theory for Unsteady Cavity Flows", Journal of Basic Engineering, Trans. ASME, Series D, Vol. 89, December 1967.
16. J. H. Kim, "The Wall Effect for Unsteady, Choked Supercavitating Flow", California Institute of Technology, Division of Engineering and Applied Science Report No. E-79A.13, January 1971.

List of Figure Captions

- Fig. 1 Sketch showing a cavitating flat plate in a choked tunnel.
- Fig. 2 Description of harmonic oscillatory motion of the hydrofoil.
- Fig. 3 Diagram for the physical z -plane showing boundary conditions for the linearized flow corresponding to Fig. 1.
- Fig. 4 Boundary conditions in the auxiliary ζ -plane.
- Fig. 5 Unsteady part of the pressure at upstream infinity normalized with respect to the apparent change in the angle of attack.
- Fig. 6(a) Normalized force coefficients for heaving.
- Fig. 6(b) Normalized moment coefficients for heaving.
- Fig. 7(a) Normalized force coefficients for pitching.
- Fig. 7(b) Normalized moment coefficients for pitching.

Appendix I

Integrals J_1 , J_2 , J_3 and J_4

A. Convergence

Integral J_1

From Equation (52), one can estimate

$$|J_1| \leq \frac{1}{\pi} \int_0^\infty \left(\frac{r-a}{2}\right)^{1/2} \left| \int_{-1}^0 g(\xi) \frac{\xi d\xi}{\xi^2 + \eta^2} \frac{dx}{d\eta} \right| d\eta$$

It is sufficient to examine the asymptotic behavior of

$$M_1(\eta) = \left(\frac{r-a}{2}\right)^{1/2} \int_{-1}^0 g(\xi) \frac{\xi d\xi}{\xi^2 + \eta^2} \frac{dx}{d\eta}$$

near $\eta=0$ and $\eta=\infty$. Note that the inner integral converges for all values of η .

Near $\eta=0$: It is easy to show that $\left(\frac{r-a}{2}\right)^{1/2}$ is $O(\eta^{-1/2})$ as $\eta \rightarrow 0$. Also from the mapping, $\frac{dx}{d\eta} \sim O(\eta)$ as $\eta \rightarrow 0$. Therefore $M_1(\eta) \sim O(\eta^{1/2})$ as $\eta \rightarrow 0$ and is integrable.

Near $\eta=\infty$: $\left(\frac{r-a}{2}\right)^{1/2}$ is found to be $O(\eta)$, and $\frac{dx}{d\eta}$ behaves like $O(\eta^{-1})$ as $\eta \rightarrow \infty$ so that $M_1 \sim O(\eta^{-2})$ as $\eta \rightarrow \infty$ and is integrable. J_1 is thus convergent.

Integral J_2

Equation (53) enables us to write

$$|J_2| \leq \frac{1}{\pi} \int_0^\infty \left(\frac{r+a}{2}\right)^{1/2} \left| \int_{-1}^0 g(\xi) \frac{\eta d\xi}{\xi^2 + \eta^2} \frac{dx}{d\eta} \right| d\eta$$

Let us examine the asymptotic behavior of

$$M_2(\eta) = \left(\frac{r+a}{2}\right)^{1/2} \int_{-1}^0 g(\xi) \frac{\eta d\xi}{\xi^2 + \eta^2} \frac{dx}{d\eta}$$

Near $\eta = 0$: $\left(\frac{r+a}{2}\right)^{1/2}$ can be shown to be $O(\eta^{-1/2})$ as $\eta \rightarrow 0$. From the mapping, $\frac{dx}{d\eta} \sim O(\eta)$ as $\eta \rightarrow 0$ so that $M_2(\eta) \sim O(\eta^{3/2})$ and is integrable.

Near $\eta = \infty$: $\left(\frac{r+a}{2}\right)^{1/2} \sim O(1)$, whereas $\frac{dx}{d\eta} \sim O(\eta^{-1})$ as $\eta \rightarrow \infty$ so that $M_2(\eta) \sim O(\eta^{-2})$ as $\eta \rightarrow \infty$ and therefore is integrable. Thus J_2 converges.

Integrals J_{3a} , J_{3b} , J_{4a} , J_{4b}

From the transformation, it can be easily shown that $x(\xi)$ is continuous and continuously differentiable for $-1 \leq \xi \leq 0$. This guarantees the convergence of these integrals by comparing them with J_1 and J_2 , and applying the same argument as was used for J_1 and J_2

B. Numerical Procedure

For each value of η , the inner integrals are numerically integrated by the Chebyshev-Gauss quadrature formula. For example,

$$L_1 = \int_{-1}^0 g(\xi) \frac{\xi d\xi}{\xi^2 + \eta^2}$$

can be converted by change of variable $\tau = 2\xi + 1$ into

$$L_1 = -2 \int_{-1}^1 \frac{1}{\sqrt{1-\tau^2}} f_1(\tau) d\tau$$

where
$$f_1(\tau) = \frac{(1-\tau)^2}{\sqrt{(1+2c_1-\tau)(\tau-1-2c_2)} [(1-\tau)^2 + \eta^2]}$$

Then

$$L_1 \approx -2 \frac{\pi}{n} \sum_{j=1}^n f_1(a_j)$$

where

$$a_j = \cos \frac{(2j-1)\pi}{2n}, \quad j = 1, 2, \dots, n$$

The following integrals are obtained in the same way:

$$L_2 = \int_{-1}^0 g(\xi) \frac{d\xi}{\xi^2 + \eta^2}$$

$$L_3 = \int_{-1}^0 g(\xi) x(\xi) \frac{\xi d\xi}{\xi^2 + \eta^2}$$

$$L_4 = \int_{-1}^0 g(\xi) x(\xi) \frac{\eta d\xi}{\xi^2 + \eta^2}$$

and two more such integrals that involve $x^2(\xi)$ in the integrand.

Now the outer integrals are evaluated by means of Simpson's rule applied for the real and the imaginary parts of the integrals. For example, write

$$J_1 = J_{1r} + jJ_{1i}$$

where

$$J_{1r} = -\frac{1}{\pi} \int_0^{\infty} \left(\frac{r-a}{2}\right)^{1/2} \int_{-1}^0 g(\xi) \frac{\xi d\xi}{\xi^2 + \eta^2} \cos kx \frac{dx}{d\eta} d\eta$$

and

$$J_{1i} = -\frac{1}{\pi} \int_0^{\infty} \left(\frac{r-a}{2}\right)^{1/2} \int_{-1}^0 g(\xi) \frac{\xi d\xi}{\xi^2 + \eta^2} \sin kx \frac{dx}{d\eta} d\eta$$

J_{1r} can be written

$$J_{1r} = T_N + E_N$$

where

$$T_N = -\frac{1}{\pi} \int_0^N \left(\frac{r-a}{2}\right)^{1/2} \int_{-1}^0 g(\xi) \frac{\xi d\xi}{\xi^2 + \eta^2} \cos kx \frac{dx}{d\eta} d\eta$$

and

$$E_N = -\frac{1}{\pi} \int_N^{\infty} \left(\frac{r-a}{2}\right)^{1/2} \int_{-1}^0 g(\xi) \frac{\xi d\xi}{\xi^2 + \eta^2} \cos kx \frac{dx}{d\eta} d\eta$$

The inner integral L_1 having been calculated for each value of η , T_N can be obtained by Simpson's formula. If η is large, asymptotic behavior of

$$\left(\frac{r-a}{2}\right)^{1/2} \int_{-1}^0 g(\xi) \frac{\xi d\xi}{\xi^2 + \eta^2} \cos kx \frac{dx}{d\eta}$$

can be found, and using this expression in the integrand for E_N , the approximate bound for E_N is obtained for large N . N is increased until it is so large that finally

$$\left| \frac{E_N}{T_N} \right| < \epsilon$$

is satisfied, ϵ being a desired tolerance in error. Then $T_N \cong J_{1r}$. The same procedure is applied for J_{1i} . The integrals $J_2, J_{3a}, J_{3b}, J_{4a}, J_{4b}$ are obtained in a similar manner.

Appendix 2

Integrals in \tilde{C}_f and \tilde{C}_m

A. Convergence

In view of Equations (66), (67) and (12), and noting that $x(\xi)$ is continuous and continuously differentiable for $-1 \leq \xi \leq 0$, it is sufficient to investigate the convergence of an integral of the form

$$M = \int_{-1}^0 \frac{f_2(\xi)}{g(\xi)} \oint_{-1}^0 \frac{g(\tau)}{\tau - \xi} f_1(\tau) d\tau \frac{dx}{d\xi} d\xi \quad (A-1)$$

$f_1(\xi)$, $f_2(\xi)$ representing any functions continuous and continuously differentiable for $-1 \leq \xi \leq 0$.

Write

$$M = \int_{-1}^0 m(\xi) d\xi \quad (A-2)$$

where

$$m(\xi) = \frac{f_2(\xi)}{g(\xi)} \oint_{-1}^0 \frac{g(\tau)}{\tau - \xi} f_1(\tau) d\tau \cdot \frac{dx}{d\xi} \quad (A-3)$$

We will show that $m(\xi)$ is continuous for $-1 \leq \xi \leq 0$.

Let

$$l(\xi) = \oint_{-1}^0 \frac{g(\tau)}{\tau - \xi} f_1(\tau) d\tau \quad (A-4)$$

and consider

(i) $-1 < \xi < 0$

In this interval, set

$$l(\xi) = l_1(\xi) + l_2(\xi) \quad (A-5)$$

where

$$l_1(\xi) = \int_{-1}^0 \frac{g(\tau)f_1(\tau) - g(\xi)f_1(\xi)}{\tau - \xi} d\tau \quad (\text{A-6})$$

and

$$l_2(\xi) = g(\xi)f_1(\xi) \oint_{-1}^0 \frac{d\tau}{\tau - \xi} \quad (\text{A-7})$$

$l_1(\xi)$ exists in the Riemann sense because the integrand is continuous throughout the interval of integration. Note that for $\tau = \xi$, the integrand becomes $\frac{d}{d\xi}(g(\xi)f_1(\xi))$ which exists.

Also, it can be shown that

$$l_2(\xi) = g(\xi)f_1(\xi) \log \left| \frac{\xi}{\xi+1} \right| \quad \text{for } -1 < \xi < 0 \quad (\text{A-8})$$

Equations (A-3) through (A-8) gives

$$m(\xi) = \frac{f_2(\xi)}{g(\xi)} \left(l_1(\xi) + g(\xi)f_1(\xi) \log \left| \frac{\xi}{\xi+1} \right| \right) \frac{dx}{d\xi} \quad (\text{A-9})$$

Therefore $m(\xi)$ is shown to be continuous for $-1 < \xi < 0$. Now we have only to consider the behavior of $m(\xi)$ near $\xi = -1$ and $\xi = 0$.

(ii) $\xi = 0$

Using Equation (16), one finds $\frac{1}{g(\xi)} \frac{dx}{d\xi} = 0$ at $\xi = 0$. Also it can be easily shown that

$$l(0) = \int_{-1}^0 \frac{g(\tau)f_1(\tau)}{\tau} d\tau$$

is bounded. Therefore, $m(0) = 0$ from Equation (A-3).

(iii) $\xi = -1$

From the behavior of Cauchy integrals near ends of the line of integration⁽¹¹⁾, it can be deduced that

$$l(\xi) = \frac{\cot \frac{\pi}{2}}{2i} \frac{\zeta^*(-1)}{(\xi+1)^{1/2}} + l^*(\xi) \quad \text{as } \xi \rightarrow -1 \quad (\text{A-10})$$

Here $l^*(\xi) = l^{**}(\xi)/|\xi+1|^\gamma$, $\gamma < 1/2$, and $l^{**}(\xi)$ satisfies the Hölder condition near and at $\xi = -1$, and

$$\zeta^*(-1) = \sqrt{\frac{-1}{(-1-c_1)(-1-c_2)}} f_1(-1)$$

Equations (A-3) and (A-10) show that

$$\lim_{\xi \rightarrow -1} m(\xi) = 0$$

Therefore $m(\xi)$ is continuous and integrable in the interval $-1 \leq \xi \leq 0$.

B. Numerical Procedure

Again, in view of Equations (66), (67) and (12), we may consider the integral of the form of Equation (A-1), in which $f_1(\tau)$ could be a constant, $x(\tau)$, or $x^2(\tau)$, and $f_2(\xi)$ could be a constant or $x(\xi)$. Dividing the interval $[-1, 0]$ into n equal subintervals and labelling $\xi_m = -1 + m\Delta\xi$, $m = 0, 1, 2, \dots, n$, where $\Delta\xi = \frac{1}{n}$, we need to compute $m(\xi_i)$. Note that $m(-1) = m(0) = 0$ from the discussion on the convergence and so we need $m(\xi_i)$ only for $1 \leq i \leq n-1$.

Consider the inner integral

$$l(\xi_i) = \int_{-1}^0 \frac{g(\tau)f_1(\tau)}{\tau - \xi_i} d\tau$$

It can be rewritten

$$l(\xi_i) = \int_{-1}^{-1+\epsilon} \frac{g(\tau)f_1(\tau)}{\tau - \xi_i} d\tau + \int_{-1+\epsilon}^0 \frac{g(\tau)f_1(\tau) - g(\xi_i)f_1(\xi_i)}{\tau - \xi_i} d\tau + g(\xi_i)f_1(\xi_i) \log \frac{-\xi_i}{1+\xi_i-\epsilon} \quad (\text{A-11})$$

If ϵ is taken so small as to allow ξ_1 to lie outside the interval $[-1, -1+\epsilon]$,

the integrand of the first integral is singular only at $\tau = -1$ for all ξ_i , $1 \leq i \leq n-1$, and this singularity contributed by $g(\tau)$ behaves like $(\tau+1)^{-1/2}$. Therefore, the first integral can be numerically carried out by the formula⁽¹²⁾.

$$\int_{-1}^{-1+\epsilon} \frac{g(\tau)f_1(\tau)}{\tau-\xi_i} d\tau \cong \frac{\epsilon}{2} \left[\frac{8\sqrt{2}}{3} g\left(-1+\frac{\epsilon}{2}\right) f_1\left(-1+\frac{\epsilon}{2}\right) / \left(-1+\frac{\epsilon}{2}-\xi_i\right) - \frac{4}{3} g(-1+\epsilon) f_1(-1+\epsilon) / (-1+\epsilon-\xi_i) \right], \quad i = 1, 2, \dots, n-1 \quad (\text{A-12})$$

The second integral in Equation (A-11) is integrable in the ordinary sense for all ξ_i , $1 \leq i \leq n-1$. When $\tau = \xi_i$, the integrand becomes

$$\frac{d}{d\xi} [g(\xi) f_1(\xi)]_{\xi=\xi_i}$$

and does exist, enabling one to use Simpson's rule.

Using Equations (A-11), (A-12) and (A-3), $m(\xi_i)$, $1 \leq i \leq n-1$, are obtained. Then Simpson's rule can be applied to evaluate

$$M = \int_{-1}^0 m(\xi) d\xi$$

Table 1. Choked Cavity Number for the Case of $h_1 = h_2 = h$ at Various Angles of Attack

	σ (Choked Cavity Number)				
h	$\alpha = 2^\circ$	$\alpha = 4^\circ$	$\alpha = 6^\circ$	$\alpha = 8^\circ$	$\alpha = 10^\circ$
1	0.0794	0.1686	0.2694	0.3839	0.5145
1.25	0.0679	0.1430	0.2262	0.3189	0.4225
2	0.0501	0.1040	0.1621	0.2250	0.2932
2.5	0.0437	0.0904	0.1402	0.1935	0.2507
4	0.0333	0.0683	0.1051	0.1438	0.1847
5	0.0294	0.0601	0.0923	0.1259	0.1611
6	0.0266	0.0543	0.0831	0.1132	0.1445
8	0.0228	0.0464	0.0708	0.0961	0.1223
10	0.0203	0.0411	0.0627	0.0849	0.1078

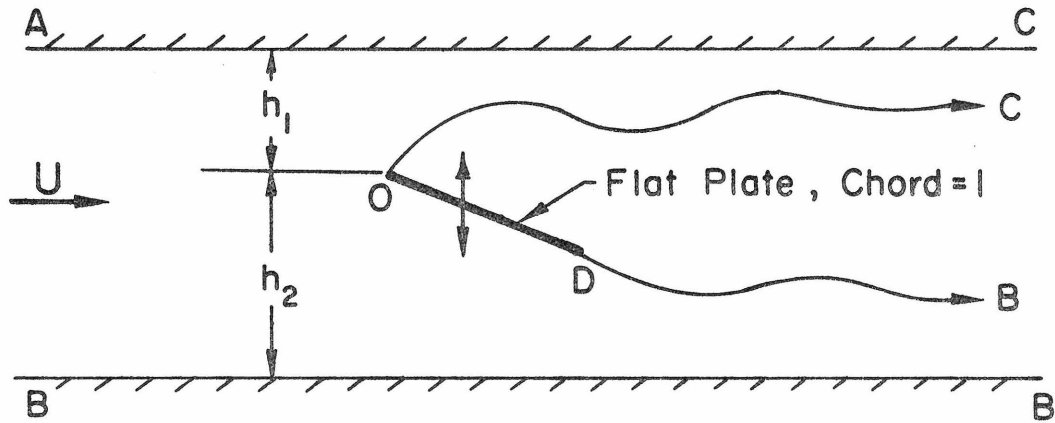


Fig. 1 Sketch showing a cavitating flat plate in a choked tunnel.

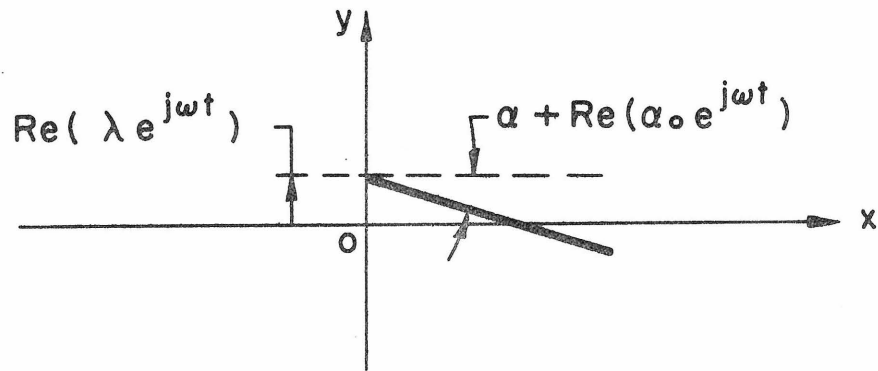


Fig. 2 Description of harmonic oscillatory motion of the hydrofoil.

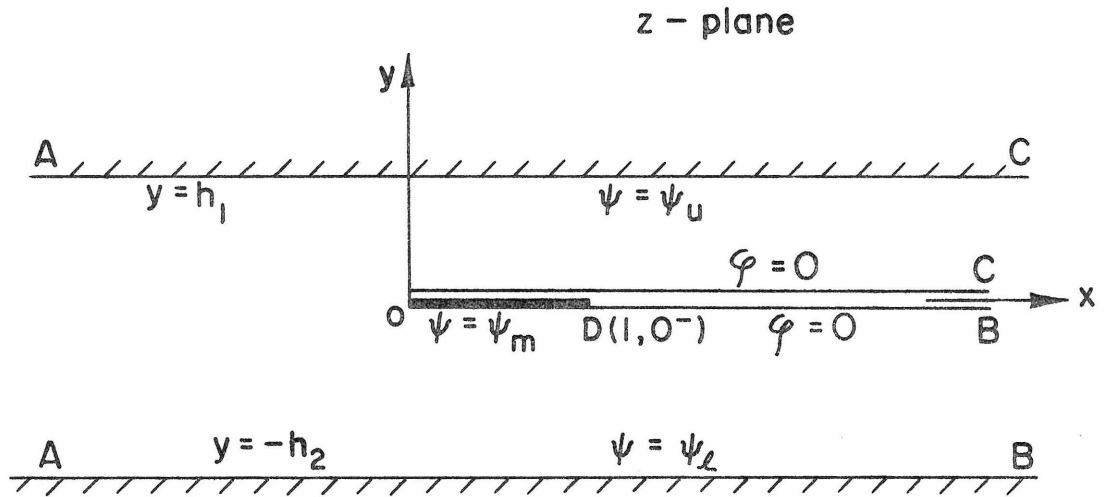


Fig. 3 Diagram of the physical z-plane showing boundary conditions for the linearized flow corresponding to Figure 1.

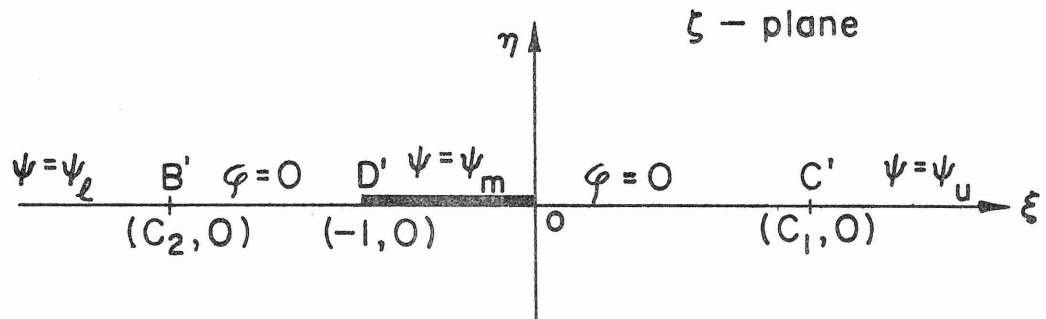


Fig. 4 Boundary conditions in the auxiliary ζ-plane.

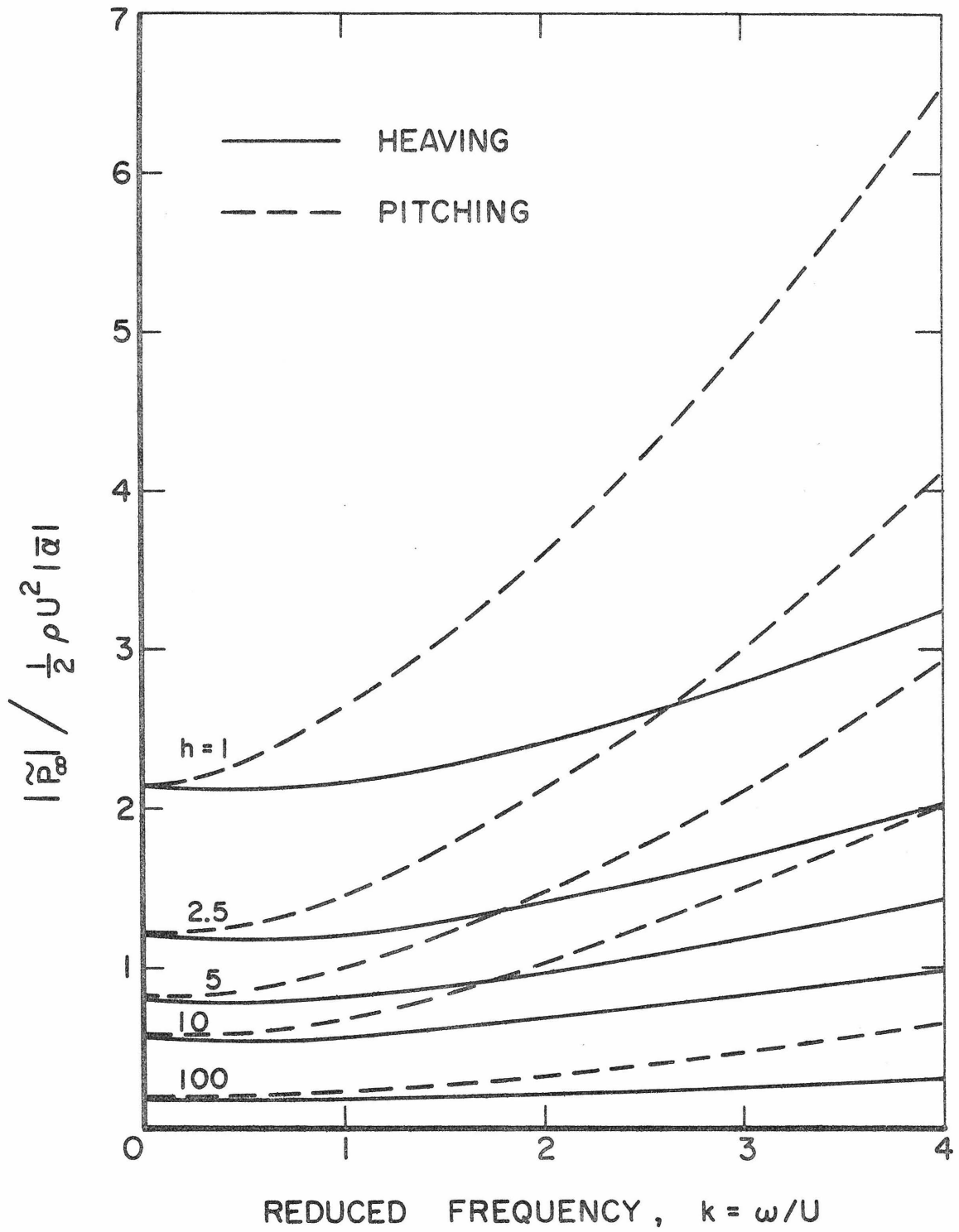


Fig. 5 Unsteady part of the pressure at upstream infinity normalized with respect to the apparent change in the angle of attack.

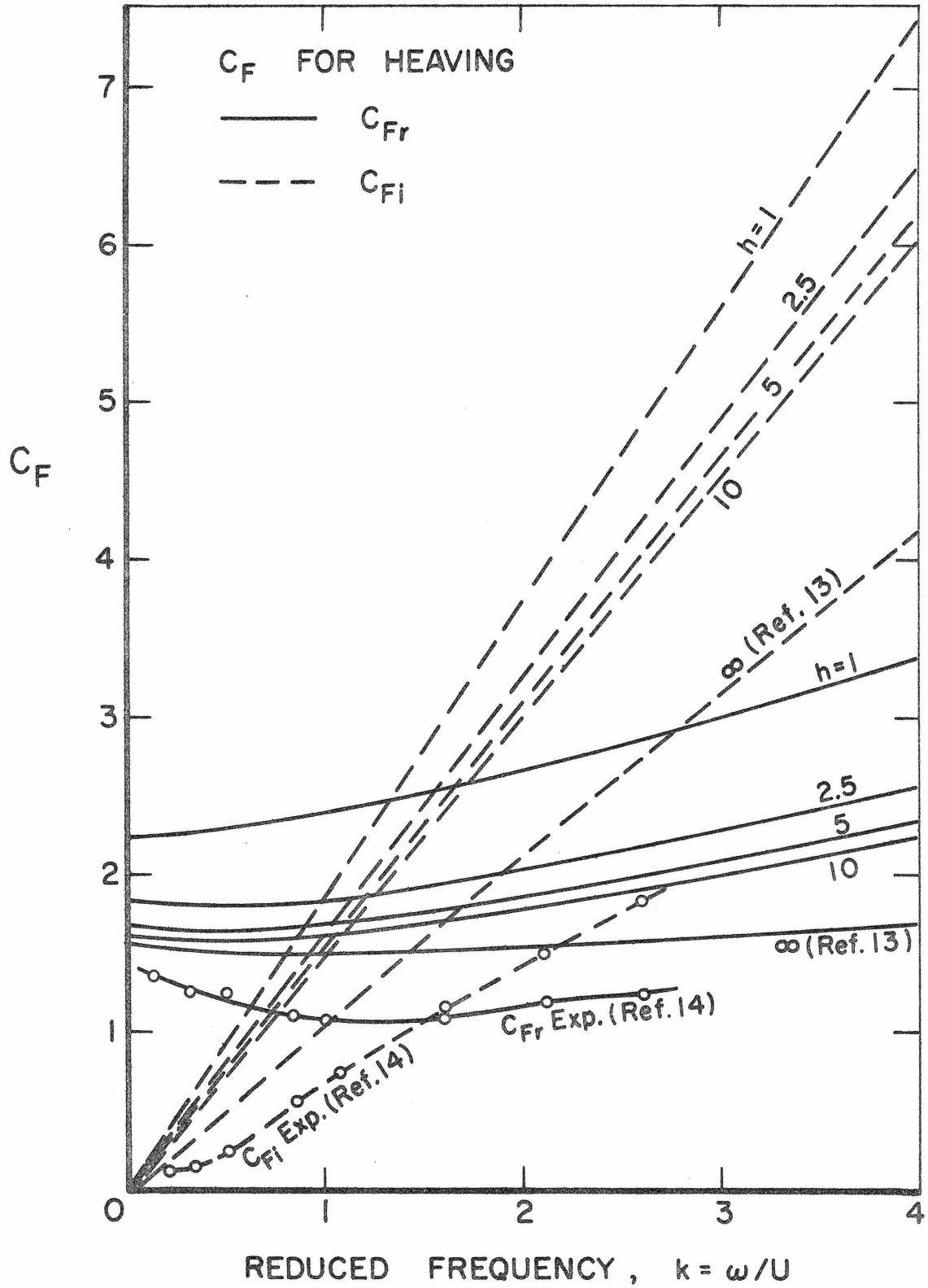


Fig. 6(a) Normalized force coefficients for heaving.

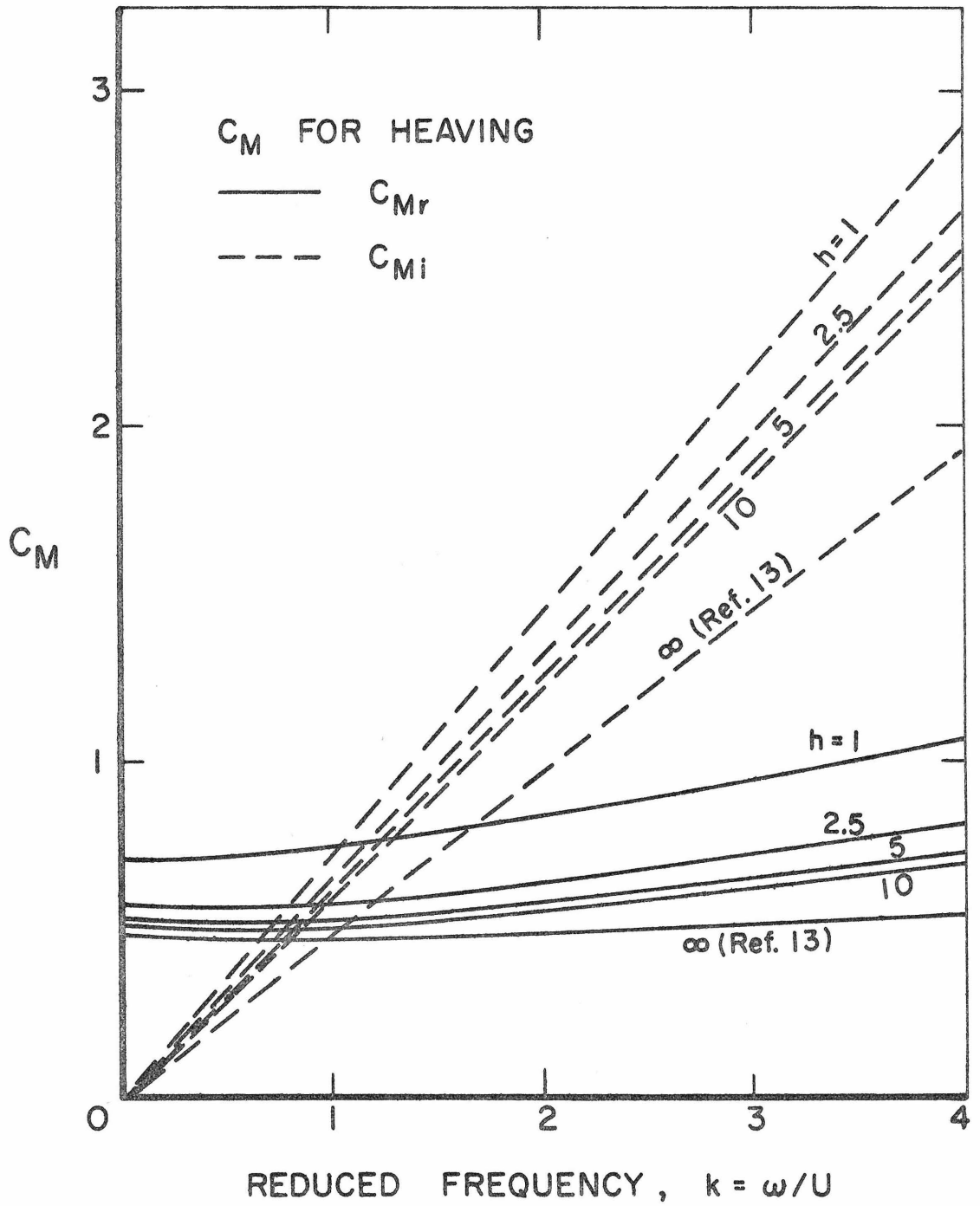


Fig. 6(b) Normalized moment coefficients for heaving.

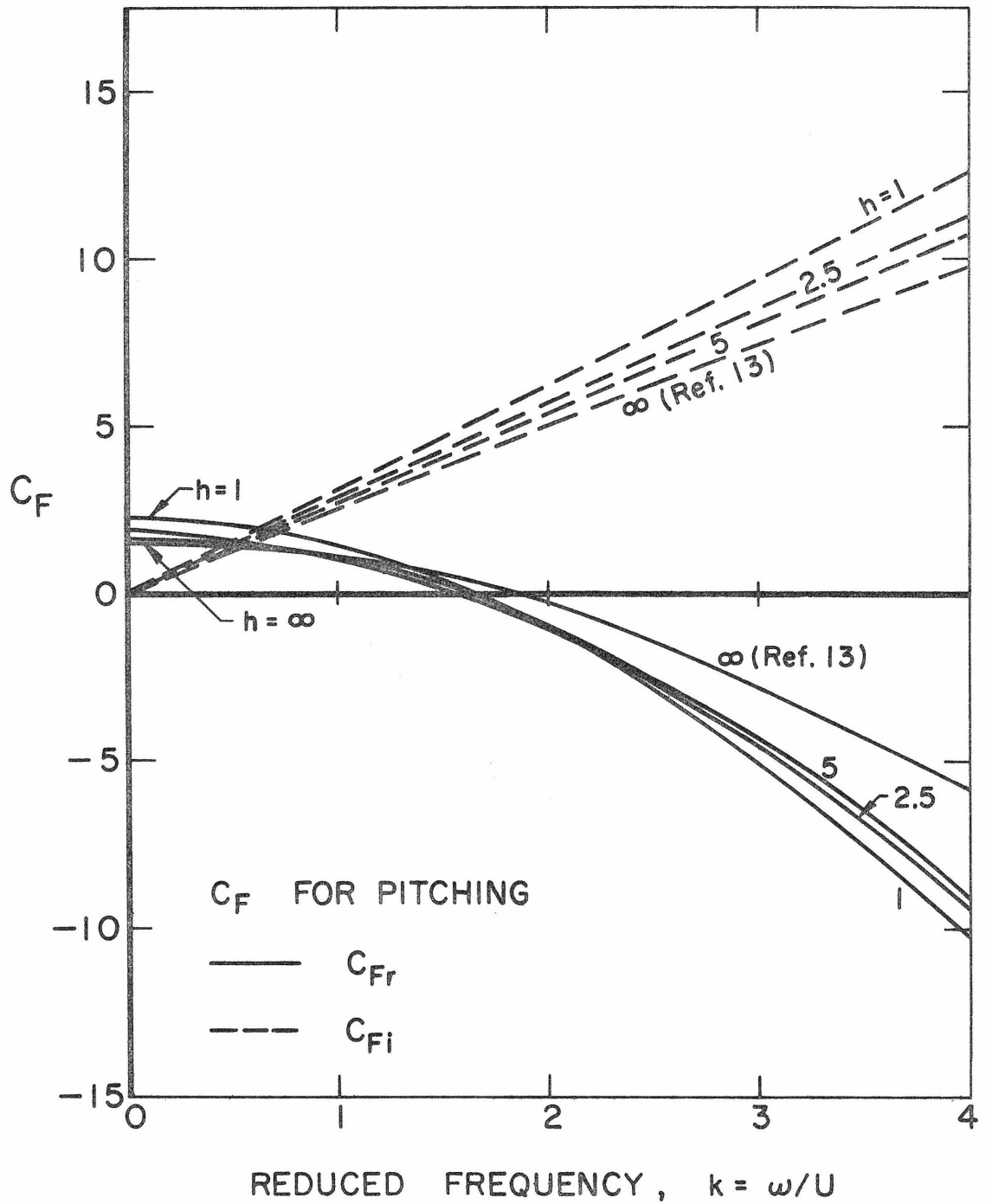


Fig. 7(a) Normalized force coefficients for pitching.

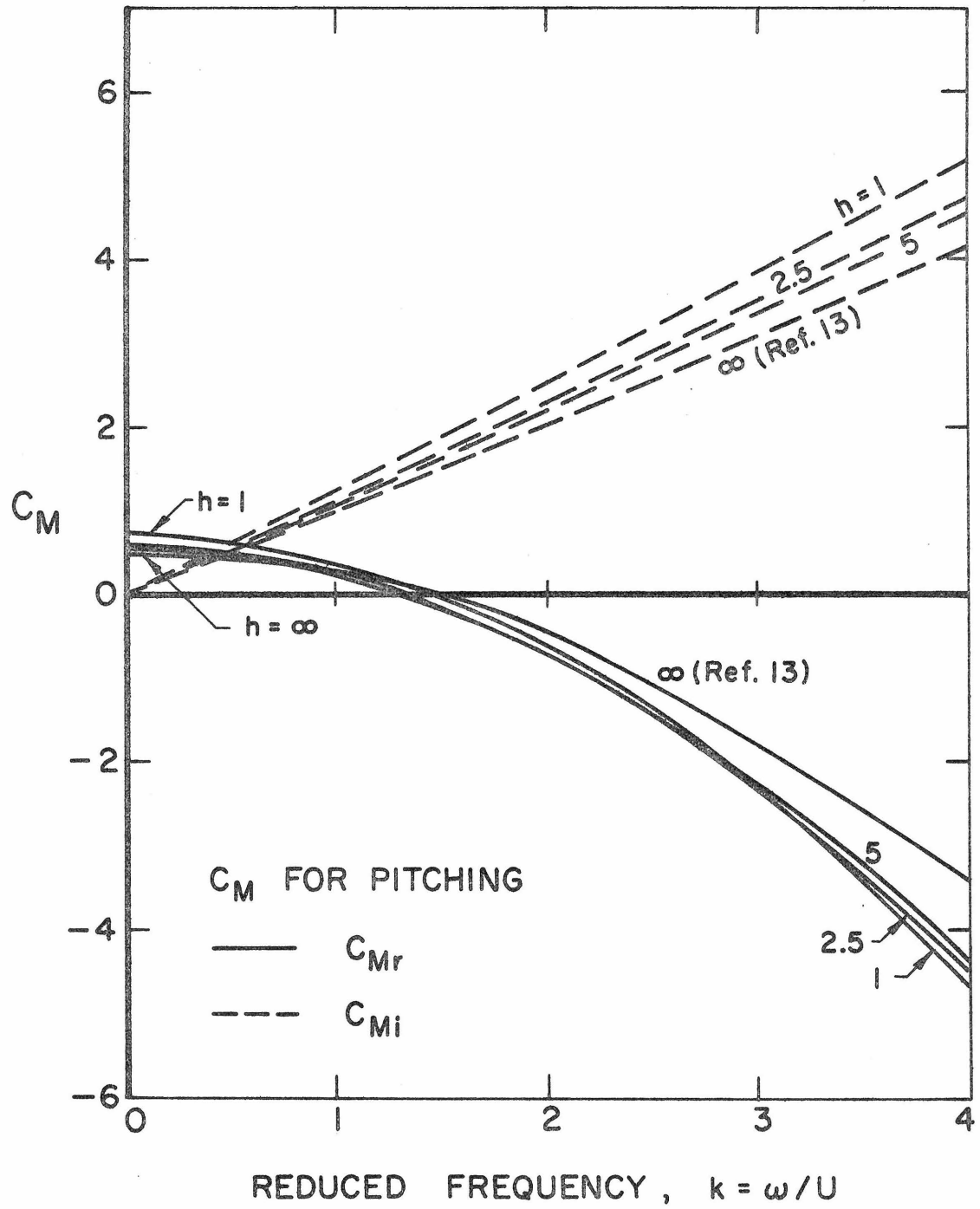


Fig. 7(b) Normalized moment coefficients for pitching.

PART II

THE CAVITATING INTERNAL FLOW
WITH MASS OSCILLATIONS

1. Introduction

Experimental studies^(1,2) of cavitating hydrofoils reveal that the basic cavitation process itself is an inherently unsteady phenomenon. So-called natural steady cavity flows are steady only in an average sense.

In an infinite fluid medium, the unsteady phenomenon for the hydrofoil is believed to be associated solely with the intrinsic nature of cavitation. In a complete hydraulic system subject to cavitation, the dynamics of the liquid motion in the piping of the system may be coupled with that contributed by the cavitation itself.

As a first step toward the study of this rather complicated hydraulic system, it is interesting to consider the following simple model situation in a water tunnel as a representative problem:

Imagine a two-dimensional tunnel of finite length with a wedge placed in the middle. Suppose that at the upstream and downstream ends the unsteady pressures are known and controlled. These pressures could correspond to the inlet and the outlet pressures in a complete turbopump. These pressure fluctuations cause a mass oscillation of known quantity even in the absence of cavity. This model may represent a most simplified version of a hydraulic system. In the presence of a cavity, there will be a coupling effect between the system and the cavity. The effect of the cavity on the remainder of the tunnel can be viewed as a time-dependent source.

Now, we can treat this problem by fictitiously extending the finite tunnel to infinity, thereby obtaining an idealized situation with all the conditions of the finite system incorporated. This is our problem at hand to be studied. The net mass fluctuation in the channel is an

undetermined quantity because the added mass oscillation due to the cavity volume change is not known beforehand. The pressure at the upstream and the downstream infinity become singular. However, this is only a formal mathematical concept and will not cause trouble since our interest is centered around the finite part of the tunnel that corresponds to the original finite system and what happens in the fictitious portion of the tunnel is not important.

2. Formulation of the Problem

Consider a wedge of unit length and half apex angle γ placed in the middle of a two-dimensional tunnel of height $2h$. The origin of the coordinates is taken at the nose of the wedge with the x -axis parallel to the walls and the y -axis orthogonal to them. In the absence of the wedge, the basic velocity field is assumed to be uniform and given by $U + \tilde{U}_0 e^{j\omega t}$ where $|\tilde{U}_0|/U \ll 1$, the mass fluctuation being possibly caused by a piston action at upstream infinity. Here j is a unit imaginary number, and it is to be understood that here and in what follows only the real part of any oscillatory quantity is to be taken, namely, $\tilde{A}e^{j\omega t} \equiv \text{Re}(\tilde{A}e^{j\omega t})$, etc.

Suppose that the wedge is held at zero angle of attack to the oncoming flow and a cavity develops from the two rear corners of the triangular body, terminating at $x = \ell(t)$. Let us assume that the pressures at $x = x_1$ upstream and $x = x_2$ downstream are specified as follows, where $h/|x_1| \ll 1$ and $\ell(t)/x_2 \ll 1$:

$$P_1 = P_{s1} + \tilde{P}_1 e^{j\omega t} \quad \text{at} \quad x = x_1$$

and

$$P_2 = P_{s2} + \tilde{P}_2 e^{j\omega t} \quad \text{at} \quad x = x_2 ,$$

where the subscript s refers to the steady condition. Similarly, the pressure on the cavity is assumed to be known

$$P = P_c + \tilde{P}_c e^{j\omega t}$$

independent of x . We will neglect the variation of the pressures at $x=x_1$ and $x=x_2$ in the y -direction under the assumption that $|x_1|$ and x_2 are sufficiently large. We may also argue that $P_{s1} \cong P_{s2} \cong P_\infty$ where P_∞ is the steady pressure at infinity. However, this approximation is immaterial for our analysis insofar as they are known from the steady system. These pressures may be regarded as the inlet and the outlet pressures of a turbomachine.

Because of the cavity volume change in time, the cavity will be viewed as a source when observed from far away. Consequently, the velocity at upstream infinity is no more given by $U + \tilde{U}_0 e^{j\omega t}$ but it has to be modified to give $U + \tilde{U} e^{j\omega t}$, where now \tilde{U} is not known a priori and it includes the effect of the cavity. However, we will still maintain $|\tilde{U}|/U \ll 1$ if the cavity volume change is small. The whole situation is illustrated in Fig. 1(a) and Fig. 1(b).

Now, let $\vec{q} = (U+u, v)$ be the velocity vector, where u and v are the perturbation velocity components in the x - and the y -direction respectively. Let us assume the flow is incompressible, inviscid and irrotational. The equation of continuity can be written

$$\frac{\partial u}{\partial x} = \frac{\partial (-v)}{\partial y}$$

The condition of irrotationality gives

$$\frac{\partial u}{\partial y} = \frac{\partial v}{\partial x}$$

The above Cauchy-Riemann relation allows one to define the complex

perturbation velocity $W(z, t) = u(x, y, t) - iv(x, y, t)$ as an analytic function of $z = x + iy$ at every instant of time t .

Assuming that $|u|/U, |v|/U \ll 1$, we may write the x-component of the Euler's equations linearized in the perturbation velocity quantities as

$$\frac{\partial u}{\partial t} + U \frac{\partial u}{\partial x} = -\frac{1}{\rho} \frac{\partial P}{\partial x}, \quad (1)$$

where P is the pressure and ρ is the fluid density.

The symmetry of the flow enables us to consider only the upper half of the field. As usual in linear theories, we will represent the cavity-wedge by a thin slit along the real axis. We are going to set up the boundary conditions for $W(z, t)$ in the upper half of the flow field. In deriving these boundary conditions, we will neglect the terms of higher order than linear in the quantities u, v and γ assuming that γ is also small.

Then on the wedge we obtain

$$v = \gamma U$$

On the cavity boundary, Equation (1) gives

$$\frac{\partial u}{\partial t} + U \frac{\partial u}{\partial x} = 0 \quad (2)$$

Let us write $u = u_c + \tilde{u}_c(x)e^{j\omega t}$ on the cavity, where u_c is the constant velocity on the cavity determined from the steady condition. In fact, u_c can be found from the Bernoulli equation for the steady flow

$$P_\infty + \frac{1}{2} \rho U^2 = P_c + \frac{1}{2} \rho [(U + u_c)^2 + v^2]$$

To first order in the perturbation quantities, we therefore obtain

$$u_c = \frac{1}{2} \sigma U \quad (3)$$

where σ is the cavitation number defined by

$$\sigma = \frac{P_{\infty} - P_c}{\frac{1}{2} \rho U^2} \quad (4)$$

Equation (2) now results in

$$j\omega \tilde{u}_c + U \frac{d\tilde{u}_c}{dx} = 0,$$

the solution of which is

$$\tilde{u}_c = \tilde{g} e^{-j \frac{\omega}{U} x} \quad (5)$$

\tilde{g} is a complex constant to be determined later.

Thus, we have established the following linearized boundary conditions:

$$v(x, 0, t) = 0 \quad x < 0 \quad (6.a)$$

$$v(x, 0, t) = \gamma U \quad 0 < x < 1 \quad (6.b)$$

$$u(x, 0, t) = u_c + \tilde{g} e^{j\omega(t - \frac{x}{U})} \quad 1 < x < l(t) \quad (6.c)$$

$$v(x, 0, t) = 0 \quad l(t) < x \quad (6.d)$$

$$v(x, h, t) = 0 \quad -\infty < x < \infty \quad (6.e)$$

These boundary conditions in the upper half of the flow field are described in Fig. 2.

To solve the above boundary value problem, it is convenient to map the upper half of the flow region in the z -plane into the upper half of the ζ -plane ($\zeta = \xi + i\eta$) by the transformation

$$z = -\frac{h}{\pi} \log \left(1 - \frac{\zeta}{c} \right) \quad (7)$$

where

$$c = \frac{1}{1 - e^{-\pi/h}} \quad (8)$$

The end of the cavity will be mapped into $\xi = S(t)$ on the real axis by the relation

$$l(t) = -\frac{h}{\pi} \log \left(1 - \frac{S(t)}{c} \right) \quad (9)$$

The boundary conditions in the ζ -plane are shown in Figure 3.

3. Solution of the Boundary Value Problem

Define a new function $W_0(\zeta, t)$ by

$$\begin{aligned} W_0(\zeta, t) &= u_0(\xi, \eta, t) - iv_0(\xi, \eta, t) \\ &= W(z(\zeta), t) - u_c \end{aligned} \quad (10)$$

Then the boundary conditions for $W_0(\zeta, t)$ become

$$v_0(\xi, 0, t) = 0 \quad \xi < 0 \quad (11.a)$$

$$v_0(\xi, 0, t) = \gamma U \quad 0 < \xi < 1 \quad (11.b)$$

$$u_0(\xi, 0, t) = \tilde{g} e^{j\omega(t-x(\xi)/U)} \quad 1 < \xi < S(t) \quad (11.c)$$

$$v_0(\xi, 0, t) = 0 \quad S(t) < \xi \quad (11.d)$$

where

$$x(\xi) = -\frac{h}{\pi} \log \left(1 - \frac{\xi}{c} \right).$$

Continuing W_0 analytically into the lower half of the ζ -plane by requiring $W_0(\bar{\zeta}, t) = -\overline{W_0(\zeta, t)}$ yields the following results:

$$W_0^+ + W_0^- = 0 \quad \xi < 0 \quad (12.a)$$

$$W_0^+ + W_0^- = -2i\gamma U \quad 0 < \xi < 1 \quad (12.b)$$

$$W_0^+ - W_0^- = 2\tilde{g} e^{j\omega(t-x(\xi)/U)} \quad 1 < \xi < S(t) \quad (12.c)$$

$$W_0^+ + W_0^- = 0 \quad S(t) < \xi \quad (12.d)$$

in which the superscripts \pm refer to the values of W_0 on $\eta = \pm 0$. The above problem is known as a Hilbert boundary value problem and detailed discussions on such a problem may be found in Reference [3].

First consider the homogeneous problem

$$H^+ + H^- = 0 \quad \xi < 1 \quad (13.a)$$

$$H^+ - H^- = 0 \quad 0 < \xi < S(t) \quad (13.b)$$

$$H^+ + H^- = 0 \quad S(t) < \xi \quad (13.c)$$

We require the Kutta condition to be satisfied at the rear end of the wedge and also we need the desired singularity at the end of the cavity of the form $N(z - \ell(t))^{-1/2}$, where N is a real constant. This singular behavior is briefly discussed in Reference [4] for steady case and the same argument is equally applicable for unsteady flow.

From the mapping function given in Equation (7), the behavior near $z = \ell$ is found to be

$$\zeta - S(t) = M(z - \ell(t)),$$

M being a real constant. Therefore, the homogeneous solution is obtained

$$H(\zeta, t) = \sqrt{\frac{\zeta - 1}{\zeta - S(t)}}, \quad (14)$$

where the branch cuts are to be taken along the real axis for $\xi < 1$ and $\xi > S$.

Now, let us define another function $G(\zeta, t)$ by the relation

$$G(\zeta, t) = \frac{W_0(\zeta, t)}{H(\zeta, t)} \quad (15)$$

Then it follows from Equations (12) and (13) that

$$G^+ - G^- = 0 \quad \xi < 0 \quad (16.a)$$

$$G^+ - G^- = -\frac{2i\gamma U}{H^+} \quad 0 < \xi < 1 \quad (16.b)$$

$$G^+ - G^- = \frac{2\tilde{g} e^{j\omega(t-x(\xi)/U)}}{H^+} \quad 1 < \xi < S \quad (16.c)$$

$$G^+ - G^- = 0 \quad S < \xi \quad (16.d)$$

where of course

$$G^+ - G^- = \frac{W_0^+}{H^+} - \frac{W_0^-}{H^-}.$$

As in Part I, use of Plemelji's formula⁽³⁾ enables us to write

$$G(\zeta, t) = \frac{1}{2\pi i} \left(\int_0^1 -\frac{2i\gamma U}{H^+(\xi)} \frac{d\xi}{\xi - \zeta} + \int_1^S \frac{2\tilde{g} e^{j\omega(t - \frac{x(\xi)}{U})}}{H^+(\xi)} \frac{d\xi}{\xi - \zeta} \right)$$

Using this expression in Equation (15) produces

$$W_0(\zeta, t) = \frac{1}{\pi} \sqrt{\frac{\zeta-1}{\zeta-S}} \left(-\gamma U \int_0^1 \sqrt{\frac{\xi-S}{\xi-1}} \frac{d\xi}{\xi-\zeta} + \tilde{g} e^{j\omega t} \int_1^S \sqrt{\frac{S-\xi}{\xi-1}} \frac{e^{-jkx(\xi)}}{\xi-\zeta} d\xi \right) + P(\zeta) \sqrt{\frac{\zeta-1}{\zeta-S}} \quad (17)$$

From here on, we will define and use $k \equiv \frac{\omega}{U}$. The last term has been added to the solution because it does not violate any boundary condition as long as $P(\zeta)$ is a rational function with real coefficients.

Equation (10) gives

$$W(z(\zeta), t) = W_0(\zeta, t) + u_c,$$

where W_0 is given by Equation (17). The condition at upstream infinity dictates that $W \rightarrow \tilde{U} e^{j\omega t}$ as $|\zeta| \rightarrow \infty$. Also the only possible singularities should occur at the origin and at the end of the cavity. The one at the

nose of the wedge should be logarithmic⁽⁴⁾ and the other one at the cavity end should be a square root singularity. Consequently, $P(\zeta)$ cannot have a pole. Hence, we immediately deduce that

$$P(\zeta) = \tilde{U} e^{j\omega t - u_c}$$

Thus we finally obtain

$$W(z(\zeta), t) = \frac{1}{\pi} \sqrt{\frac{\zeta-1}{\zeta-S}} \left[-\gamma U \int_0^1 \sqrt{\frac{\xi-S}{\xi-1}} \frac{d\xi}{\xi-\zeta} + \tilde{g} e^{j\omega t} \int_1^S \sqrt{\frac{S-\xi}{\xi-1}} \frac{e^{-jkx(\xi)}}{\xi-\zeta} d\xi + \pi \left(\tilde{U} e^{j\omega t - u_c} \right) \right] + u_c \quad (18)$$

We now proceed to determine $S(t)$, \tilde{U} and \tilde{g} . Assuming that $l(t) = l_0 + \tilde{l} e^{j\omega t}$ where $|\tilde{l}|/l_0 \ll 1$ and $|\tilde{l}|/h \ll 1$, we are allowed to write from Equation (9),

$$S(t) = S_0 + \tilde{S} e^{j\omega t} \quad (19)$$

where

$$S_0 = c \left(1 - e^{-\frac{\pi l_0}{h}} \right) \quad (20)$$

and

$$\tilde{S} = \frac{\pi c}{h} e^{-\frac{\pi l_0}{h}} \tilde{l} \quad (21)$$

It is seen that $|\tilde{S}|/S_0 \ll 1$.

If we were further allowed to write

$$W = W_s(z) + \tilde{W}(z) e^{j\omega t} \quad (22)$$

under the assumption that all the disturbances with angular velocity different from ω are negligible, it is found that

$$W_s(z(\zeta)) = \frac{1}{\pi} \sqrt{\frac{\zeta-1}{\zeta-S_0}} \left(-\gamma U \int_0^1 \sqrt{\frac{\xi-S_0}{\xi-1}} \frac{d\xi}{\xi-\zeta} - \pi u_c \right) + u_c \quad (23)$$

and

$$\begin{aligned} \tilde{W}(z(\zeta)) = \frac{1}{\pi} \sqrt{\frac{\zeta-1}{\zeta-S_0}} \left[-\frac{\gamma U \tilde{S}}{2} \left(\frac{1}{\zeta-S_0} \int_0^1 \sqrt{\frac{\xi-S_0}{\xi-1}} \frac{d\xi}{\xi-\zeta} - \int_0^1 \frac{d\xi}{\sqrt{(\xi-1)(\xi-S_0)}(\xi-\zeta)} \right) \right. \\ \left. + \tilde{g} \int_1^{S_0} \sqrt{\frac{S_0-\xi}{\xi-1}} \frac{e^{-jkx(\xi)}}{\xi-\zeta} d\xi + \pi \left(\tilde{U} - \frac{u_c}{2} \frac{\tilde{S}}{\zeta-S_0} \right) \right] \quad (24) \end{aligned}$$

The expansion given in Equation (24) is not valid near the end of the cavity where $|\zeta-S_0| < |\tilde{S}|$. Near there, a square root singularity must be displayed as required, whereas Equation (24) exhibits a 3/2 - singularity which is not allowable.

To determine the unknowns S_0 , \tilde{S} , \tilde{U} and \tilde{g} , the following conditions are at hand:

(i) It is necessary to connect the pressure on the cavity with the pressure at $x = x_1$. Write

$$P = P_s + \tilde{P} e^{j\omega t}$$

and

$$u = u_s + \tilde{u} e^{j\omega t}$$

where P_s and u_s are the steady solutions which satisfy

$$U \frac{\partial u_s}{\partial x} = -\frac{1}{\rho} \frac{\partial P_s}{\partial x}$$

Then it follows from Equation (1) that

$$j\omega \tilde{u} + U \frac{\partial \tilde{u}}{\partial x} = -\frac{1}{\rho} \frac{\partial \tilde{P}}{\partial x} \quad (25)$$

Integrating Equation (25) from $(x_1, 0)$ to $(1, 0)$ along the real axis gives

$$\int_{x_1}^1 \left(j\omega \tilde{u} + U \frac{\partial \tilde{u}}{\partial x} \right) dx = -\frac{1}{\rho} (\tilde{P}_c - \tilde{P}_1)$$

or

$$j\omega \int_{x_1}^1 \tilde{u} dx = -\frac{1}{\rho} (\tilde{P}_c - \tilde{P}_1) - U [\tilde{u}(1, 0) - \tilde{u}(x_1, 0)] \quad (26)$$

Equation (6.c) gives

$$\tilde{u}(1, 0) = \tilde{g} e^{-j \frac{\omega}{U}}$$

Also Equation (24) gives

$$\begin{aligned} \tilde{u}(x_1, 0) = \frac{1}{\pi} \sqrt{\frac{\Lambda_1 - 1}{\Lambda_1 - S_0}} \left[-\frac{\gamma U \tilde{S}}{2} \left(\frac{1}{\Lambda_1 - S_0} \int_0^1 \frac{\sqrt{\xi - S_0}}{\xi - 1} \frac{d\xi}{\xi - \Lambda_1} - \int_0^1 \frac{d\xi}{\sqrt{(\xi - 1)(\xi - S_0)} (\xi - \Lambda_1)} \right) \right. \\ \left. + \tilde{g} \int_1^{S_0} \sqrt{\frac{S_0 - \xi}{\xi - 1}} \frac{e^{-jkx(\xi)}}{\xi - \Lambda_1} d\xi + \pi \left(\tilde{U} - \frac{u_c}{2} \frac{\tilde{S}}{\Lambda_1 - S_0} \right) \right] \quad (27) \end{aligned}$$

in which Λ_1 is calculated from Equation (7) by

$$x_1 = -\frac{h}{\pi} \log \left(1 - \frac{\Lambda_1}{c} \right)$$

or

$$\Lambda_1 = c \left(1 - e^{-\frac{\pi x_1}{h}} \right) \quad (28)$$

The integral appearing in Equation (26) is carried out along the real axis in the ζ -plane to give

$$j\omega \int_{x_1}^1 \tilde{u} dx = -\frac{h}{\pi} j\omega \int_{\Lambda_1}^1 \tilde{u}(x(\xi)) \frac{d\xi}{\xi - c} \quad (29)$$

Substituting Equation (24) into Equation (29) and using Equation (26), and the expression for $\tilde{u}(1, 0)$ given above, one arrives at

$$\begin{aligned}
 & -\frac{h}{\pi} j\omega \int_{\Lambda_1}^1 \sqrt{\frac{\xi-1}{\xi-S_0}} \left[-\frac{\gamma U \tilde{S}}{2} \left(\frac{1}{\xi-S_0} \oint_0^1 \sqrt{\frac{\tau-S_0}{\tau-1}} \frac{d\tau}{\tau-\xi} - \oint_0^1 \frac{d\tau}{\sqrt{(\tau-1)(\tau-S_0)(\tau-\xi)}} \right) \right. \\
 & \left. + \tilde{g} \int_1^{S_0} \sqrt{\frac{S_0-\tau}{\tau-1}} \frac{e^{-jkx(\tau)}}{\tau-\xi} d\tau + \pi \left(\tilde{U} - \frac{\tilde{S}}{2} \frac{u_c}{\xi-S_0} \right) \right] \frac{d\xi}{\xi-c} = -\frac{1}{\rho} (\tilde{P}_c - \tilde{P}_1) - U[\tilde{g}e^{-jk} - \tilde{u}(x_1, 0)]
 \end{aligned} \tag{30}$$

where $\tilde{u}(x_1, 0)$ is given by Equation (27) and $x(\tau)$ is given from Equation (7) as

$$x(\tau) = -\frac{h}{\pi} \log \left(1 - \frac{\tau}{c} \right)$$

In the above and in what follows, the Cauchy principal value of the integral is understood by the symbol \oint .

(ii) We use the relation between the pressures at $x=x_1$ and $x=x_2$. Integrating Equation (25) along the wall from (x_1, h) to (x_2, h) , we obtain

$$j\omega \int_{x_1}^{x_2} \tilde{u}(x, h) dx = -\frac{1}{\rho} (\tilde{P}_2 - \tilde{P}_1) - U(\tilde{u}(x_2, h) - \tilde{u}(x_1, h)) \tag{31}$$

In the ζ -plane, the line of integration will be mapped onto a portion of the positive real axis.

A similar procedure that led to obtaining Equation (30) can be applied to Equation (31) to yield

$$\begin{aligned}
 & -\frac{h}{\pi} j\omega \int_{\Lambda_2}^{\Lambda_3} \sqrt{\frac{\xi-1}{\xi-S_0}} \left[-\frac{\gamma U \tilde{S}}{2} \left(\frac{1}{\xi-S_0} \int_0^1 \sqrt{\frac{\tau-S_0}{\tau-1}} \frac{d\tau}{\tau-\xi} - \int_0^1 \frac{d\tau}{\sqrt{(\tau-1)(\tau-S_0)(\tau-\xi)}} \right) \right. \\
 & \left. + \tilde{g} \int_1^{S_0} \sqrt{\frac{S_0-\tau}{\tau-1}} \frac{e^{-jkx(\tau)}}{\tau-\xi} d\tau + \pi \left(\tilde{U} - \frac{u_c}{2} \frac{\tilde{S}}{\xi-S_0} \right) \right] \frac{d\xi}{\xi-c} \\
 & = -\frac{1}{\rho} (\tilde{P}_2 - \tilde{P}_1) - U(\tilde{u}(x_2, h) - \tilde{u}(x_1, h))
 \end{aligned} \tag{32}$$

where

$$\begin{aligned} \tilde{u}(x_1, h) = \frac{1}{\pi} \sqrt{\frac{\Lambda_2 - 1}{\Lambda_2 - S_0}} \left[-\frac{\gamma U \tilde{S}}{2} \left(\frac{1}{\Lambda_2 - S_0} \int_0^1 \sqrt{\frac{\xi - S_0}{\xi - 1}} \frac{d\xi}{\xi - \Lambda_2} - \int_0^1 \frac{d\xi}{\sqrt{(\xi - 1)(\xi - S_0)(\xi - \Lambda_2)}} \right) \right. \\ \left. + \tilde{g} \int_1^{S_0} \sqrt{\frac{S_0 - \xi}{\xi - 1}} \frac{e^{-jkx(\xi)}}{\xi - \Lambda_2} d\xi + \pi \left(\tilde{U} - \frac{u_c}{2} \frac{\tilde{S}}{\Lambda_2 - S_0} \right) \right] \quad (33) \end{aligned}$$

and

$$\begin{aligned} \tilde{u}(x_2, h) = \frac{1}{\pi} \sqrt{\frac{\Lambda_3 - 1}{\Lambda_3 - S_0}} \left[-\frac{\gamma U \tilde{S}}{2} \left(\frac{1}{\Lambda_3 - S_0} \int_0^1 \sqrt{\frac{\xi - S_0}{\xi - 1}} \frac{d\xi}{\xi - \Lambda_3} - \int_0^1 \frac{d\xi}{\sqrt{(\xi - 1)(\xi - S_0)(\xi - \Lambda_3)}} \right) \right. \\ \left. + \tilde{g} \int_1^{S_0} \sqrt{\frac{S_0 - \xi}{\xi - 1}} \frac{e^{-jkx(\xi)}}{\xi - \Lambda_3} d\xi + \pi \left(\tilde{U} - \frac{u_c}{2} \frac{\tilde{S}}{\Lambda_3 - S_0} \right) \right] \quad (34) \end{aligned}$$

The points $(\Lambda_2, 0)$ and $(\Lambda_3, 0)$ in the ζ -plane correspond to (x_1, h) and (x_2, h) respectively in the z -plane, that is, Λ_2 and Λ_3 are calculated from Equation (7) to be

$$\Lambda_2 = c \left(1 + e^{-\frac{\pi x_1}{h}} \right) \quad (35)$$

and

$$\Lambda_3 = c \left(1 + e^{-\frac{\pi x_2}{h}} \right) \quad (36)$$

(iii) Finally, we need the kinematic boundary condition on the cavity surface. Let $Y(x, t)$ represent the ordinate of the cavity-body. Then we must have

$$\frac{\partial Y}{\partial t} + U \frac{\partial Y}{\partial x} = v(x, 0, t) \quad (37)$$

with $Y(0, t) = 0$.

The solution is given by

$$Y(x, t) = \frac{1}{U} \int_0^x v(x', 0, t + \frac{x' - x}{U}) dx' \quad (38)$$

Now, the condition that the cavity-body should form a closed body is equivalent to the condition

$$Y(\ell(t), t) = 0$$

By use of Equation (38), this becomes

$$\int_0^{\ell(t)} v\left(x, 0, t + \frac{x - \ell(t)}{U}\right) dx = 0$$

This is the closure condition that we need.

To first approximation, the above becomes

$$\int_0^{\ell(t)} v\left(x, 0, t + \frac{x - \ell_0}{U}\right) dx = 0 \quad (39)$$

In the steady limit, this reduces to

$$\int_0^{\ell_0} v_s(x, 0) dx = 0 \quad (40)$$

where v_s is the steady solution for the y-component velocity.

If we can write the unsteady part of $v(x, 0, t)$ as $\tilde{v}(x, 0)e^{j\omega t}$, the unsteady part of Equation (39) may be picked up to give

$$\int_0^{\ell(t)} \tilde{v}(x, 0)e^{j\omega\left(t + \frac{x - \ell_0}{U}\right)} dx = 0 \quad (41)$$

Now, first look at Equation (40). We may write it as

$$-\text{Im} \int_0^{\ell_0} W_s(z) dz = 0,$$

the line of integration being along the real axis. Or, in the ζ -plane

$$\text{Im} \int_0^{S_0} W_s(z(\zeta)) \frac{d\zeta}{\zeta - c} = 0, \quad (42)$$

the line of integration being accordingly mapped onto the real axis of the

ζ -plane. To carry out the above integral, let us devise a contour of integration as follows:

Draw a sufficiently large semicircle of radius R centered at $\zeta=c$ and label it C_R . Also draw a sufficiently small semicircle of radius ϵ centered at $\zeta=c$ and call this C_ϵ . These semicircles drawn above the real axis and the portion of the real axis lying between them will form a closed contour. Denote this closed contour by C_0 .

Noting that on the real axis of the ζ -plane $v_s=0$ for $\xi < 0$ and $\xi > S_0$, the following equation is obtained:

$$\text{Im} \oint_{C_0} W_s(z(\zeta)) \frac{d\zeta}{\zeta-c} = \text{Im} \left(\int_0^{S_0} W_s(z(\zeta)) \frac{d\zeta}{\zeta-c} + \int_{C_\epsilon} W_s(z(\zeta)) \frac{d\zeta}{\zeta-c} + \int_{C_R} W_s(z(\zeta)) \frac{d\zeta}{\zeta-c} \right),$$

the first integral of the right hand side being carried out along the real axis.

However, we must have

$$\oint_{C_0} W_s(z(\zeta)) \frac{d\zeta}{\zeta-c} = 0$$

since the only pole at $\zeta=c$ has been deliberately indented out. Equation (42) and the above two relations imply that we must have

$$\text{Im} \left(\int_{C_\epsilon} W_s \frac{d\zeta}{\zeta-c} + \int_{C_R} W_s \frac{d\zeta}{\zeta-c} \right) = 0 \quad (43)$$

Now, substitute Equation (23) into Equation (43) and take $\epsilon \rightarrow 0$, $R \rightarrow \infty$ to obtain

$$\frac{1}{\pi} \sqrt{\frac{c-1}{c-S_0}} \left(-\gamma U \int_0^1 \sqrt{\frac{\xi-S_0}{\xi-1}} \frac{d\xi}{\xi-c} - \pi u_c \right) + u_c = 0 \quad (44)$$

This is the relation that determines S_0 . Incidentally, we can find a

closed form for the integral appearing in the above equation if desired. Remark that the same result would have been obtained from the condition $W_s(z = +\infty) = 0$. That is, $W_s(\zeta = c) = 0$ in Equation (23) would have directly produced Equation (44).

Now, let us turn to Equation (41). In the ζ -plane, this integral relation becomes

$$\int_0^{S(t)} \tilde{v}(x(\xi), 0) e^{j\omega\left(t + \frac{x(\xi) - l_0}{U}\right)} \frac{d\xi}{\xi - c} = 0 \quad (45)$$

For simplicity, we will rearrange all the phases of the unsteady quantities in such a way that \tilde{S} becomes real and positive. This does not cause any artificiality inasmuch as the phase differences between \tilde{P}_1 , \tilde{P}_2 and \tilde{P}_c are known.

Equation (45) can be split into two parts to give

$$\int_0^{S_0 - \tilde{S}} \tilde{v}(x(\xi), 0) e^{j\omega\left(t + \frac{x(\xi) - l_0}{U}\right)} \frac{d\xi}{\xi - c} + \int_{S_0 - \tilde{S}}^S \tilde{v}(x(\xi), 0) e^{j\omega\left(t + \frac{x(\xi) - l_0}{U}\right)} \frac{d\xi}{\xi - c} = 0$$

In the second integral above, we can approximate $x(\xi) - l_0 \cong 0$ because the interval of integration is near the terminus of the cavity. Thus we may write the above relation as

$$I_1 e^{-jk l_0} + I_2 = 0 \quad (46)$$

where

$$I_1 = \int_0^{S_0 - \tilde{S}} \tilde{v}(x(\xi), 0) e^{jkx(\xi)} \frac{d\xi}{\xi - c} \quad (47)$$

and

$$I_2 = \int_{S_0}^S \tilde{S}^{-1} \tilde{v}(x(\xi), 0) \frac{d\xi}{\xi - c} \quad (48)$$

For the integral I_1 , the expansion given in Equation (24) is available.

Noting that $\tilde{v}(x(\xi), 0) = 0$ for $\xi < 1$, and using Equation (24), we can write

$$I_1 = \frac{1}{\pi} \int_1^{S_0} \tilde{S}^{-1} \sqrt{\frac{\xi-1}{S_0-\xi}} \left[-\frac{\gamma U \tilde{S}}{2} \left(\frac{1}{\xi-S_0} \int_0^1 \sqrt{\frac{\tau-S_0}{\tau-1}} \frac{d\tau}{\tau-\xi} - \int_0^1 \frac{d\tau}{\sqrt{(\tau-1)(\tau-S_0)}(\tau-\xi)} \right) \right. \\ \left. + \tilde{g} \int_1^{S_0} \sqrt{\frac{S_0-\tau}{\tau-1}} \frac{e^{-jkx(\tau)}}{\tau-\xi} d\tau + \pi \left(\tilde{U} - \frac{u_c}{2} \frac{\tilde{S}}{\xi-S_0} \right) \right] \frac{e^{jkx(\xi)}}{\xi-c} d\xi \quad (49)$$

For the integral I_2 , the expansion given in Equation (24) is no longer valid because it gives a $3/2$ -singularity in the interval of integration which is not allowable. Therefore, we must use the original form of the solution given by Equation (18). If we write

$$J = \int_{S_0}^S \tilde{S}^{-1} v(x(\xi), 0, t) \frac{d\xi}{\xi - c} \quad (50)$$

and put $J = J_s + \tilde{J}e^{j\omega t}$, then clearly $\tilde{J} = I_2$ by comparing Equations (48) and (50). The idea is to evaluate Equation (50) and extract the unsteady part from it rather than to evaluate I_2 by Equation (48).

Now, Equation (18) is substituted into Equation (50) to yield

$$J = \frac{1}{\pi} \int_{S_0}^S \tilde{S}^{-1} \sqrt{\frac{\xi-1}{S_0-\xi}} \left[-\gamma U \int_0^1 \sqrt{\frac{\tau-S_0}{\tau-1}} \frac{d\tau}{\tau-\xi} \right. \\ \left. + \tilde{g} e^{j\omega t} \int_1^S \sqrt{\frac{S_0-\tau}{\tau-1}} \frac{e^{-jkx(\tau)}}{\tau-\xi} d\tau + \pi \left(\tilde{U} e^{j\omega t} - u_c \right) \right] \frac{d\xi}{\xi - c} \quad (51)$$

Let us define the integrand by

$$f(\xi) = \frac{\sqrt{\xi-1}}{\xi-c} \left[-\gamma U \int_0^1 \sqrt{\frac{\tau-S_0}{\tau-1}} \frac{d\tau}{\tau-\xi} + \tilde{g} e^{j\omega t} \int_1^S \sqrt{\frac{S_0-\tau}{\tau-1}} \frac{e^{-jkx(\tau)}}{\tau-\xi} d\tau + \pi \left(\tilde{U} e^{j\omega t} - u_c \right) \right]$$

Then Equation (51) may be written

$$J = \frac{1}{\pi} \int_{S_0 - \tilde{S}}^S \frac{f(\xi)}{\sqrt{S - \xi}} d\xi$$

Since the interval of integration is small, we can approximate the above as

$$J \cong \frac{f(S_0)}{\pi} \int_{S_0 - \tilde{S}}^S \frac{d\xi}{\sqrt{S - \xi}} = \frac{2f(S_0)}{\pi} \sqrt{\tilde{S}(1 + e^{j\omega t})} \quad (52)$$

Using the definition of $f(S_0)$ in Equation (52) then allows us to write

$$J \cong \frac{2}{\pi} \frac{\sqrt{S_0 - 1}}{S_0 - c} \sqrt{\tilde{S}(1 + e^{j\omega t})} \left[-\gamma U \int_0^1 \frac{\sqrt{\tau - S}}{\sqrt{\tau - 1} \tau - S_0} d\tau + \tilde{g} e^{j\omega t} \int_1^S \frac{\sqrt{S - \tau}}{\sqrt{\tau - 1} \tau - S_0} e^{-jkx(\tau)} d\tau + \pi (\tilde{U} e^{j\omega t} - u_c) \right] \quad (53)$$

From the above, we are going to extract only those terms containing $e^{j\omega t}$. First, define a function $f_1(\theta)$ by

$$f_1(\theta) = \sqrt{1 + \text{Re } e^{j\theta}} = \sqrt{1 + \cos \theta}$$

where $\theta = \omega t$. Expanding $f_1(\theta)$ in a Fourier series, we find that

$$f_1(\theta) = \frac{2\sqrt{2}}{\pi} \left(1 + \frac{2}{3} \cos \theta \right) + \sum_{n=2}^{\infty} a_n \cos n\theta$$

or

$$\sqrt{1 + e^{j\omega t}} = \frac{2\sqrt{2}}{\pi} \left(1 + \frac{2}{3} e^{j\omega t} \right) + \sum_{n=2}^{\infty} a_n e^{jn\omega t}$$

in which only the real part is to be taken. Using the above expression in Equation (53) and expanding all the other terms appearing in Equation (53) in a power series around $\tau = S_0$, we can extract \tilde{J} which is found to be

$$\tilde{J} = \frac{4\sqrt{2}}{\pi^2} \frac{\sqrt{S_0-1}}{S_0-c} \sqrt{\tilde{S}} \left[\frac{\gamma U \tilde{S}}{2} \int_0^1 \frac{d\tau}{\sqrt{(1-\tau)(S_0-\tau)} (S_0-\tau)} \right. \\ \left. - \tilde{g} \int_1^{S_0} \frac{e^{-jkx(\tau)}}{\sqrt{(\tau-1)(S_0-\tau)}} d\tau + \pi \tilde{U} + \frac{2}{3} \left(\gamma U \int_0^1 \frac{d\tau}{\sqrt{(1-\tau)(S_0-\tau)}} - \pi u_c \right) \right] \quad (54)$$

Replacing the integral I_2 by \tilde{J} given above, Equation (46) becomes

$$I_1 e^{-jkl_0} + \tilde{J} = 0 \quad (55)$$

where I_1 and \tilde{J} are given by Equations (49) and (54) respectively.

Equations (30), (32), (44) and (55) completely determine all the unknown constants S_0 , \tilde{S} , \tilde{g} and \tilde{U} . With these constants fully determined, the complex velocity becomes known and the solution is complete.

Once the velocity field is determined, the pressure can be calculated by integrating the Euler's equation. Then the force on the wedge will be found by integrating the pressure along the wedge. Because of symmetry, only the drag force is an interesting quantity to be found.

Special Case:

The only simple case is when the cavity extends to infinity, the state known as the choked flow. In this case, \tilde{S} will vanish and $S_0 \rightarrow c$.

The source-like effect caused by the time rate of cavity volume change will be absent and accordingly the oscillatory component of the velocity at upstream infinity is given by $\tilde{U}_0 e^{j\omega t}$ which is known beforehand. Also note that the point $(x_2, 0)$ should be removed to infinity.

Now Equation (18) becomes

$$W(z(\zeta), t) = \frac{1}{\pi} \sqrt{\frac{\zeta-1}{\zeta-c}} \left[-\gamma U \int_0^1 \sqrt{\frac{\xi-c}{\xi-1}} \frac{d\xi}{\xi-\zeta} \right. \\ \left. + \tilde{g} e^{j\omega t} \int_1^c \sqrt{\frac{c-\xi}{\xi-1}} \frac{e^{-jkx(\xi)}}{\xi-\zeta} d\xi + \pi \left(\tilde{U}_0 e^{j\omega t} - u_c \right) \right] + u_c \quad (56)$$

The only unknown appearing in Equation (56) is \tilde{g} and it will be determined from the condition that at $x=x_1$ the pressure should assume the specified value. Putting $S_0 = c$, $\tilde{S} = 0$, and $\tilde{U} = \tilde{U}_0$ into Equation (30), this condition is shown to become

$$-\frac{h}{\pi} \frac{j\omega}{2} \int_{\Lambda_1}^1 \sqrt{\frac{\xi-1}{\xi-c}} \left(\tilde{g} \int_1^c \sqrt{\frac{c-\tau}{\tau-1}} \frac{e^{-jkx(\tau)}}{\tau-\xi} d\tau + \pi \tilde{U}_0 \right) \frac{d\xi}{\xi-c} \\ = -\frac{1}{\rho} \left(\tilde{P}_c - \tilde{P}_1 \right) - U \left(\tilde{g} e^{-jkx} - \tilde{u}(x_1, 0) \right) \quad (57)$$

where $\tilde{u}(x_1, 0)$ is given from Equation (27) by

$$\tilde{u}(x_1, 0) = \frac{1}{\pi} \sqrt{\frac{\Lambda_1-1}{\Lambda_1-c}} \left(\tilde{g} \int_1^c \sqrt{\frac{c-\xi}{\xi-1}} \frac{e^{-jkx(\xi)}}{\xi-\Lambda_1} d\xi + \pi \tilde{U}_0 \right) \quad (58)$$

The closure condition and the pressure condition at $x=x_2$ (where now we must have $x_2 \rightarrow \infty$) should be abandoned.

4. Discussion and Conclusion

Although some of the integrals could have been evaluated in closed forms using the table of integrals, they have been left as integral forms in order to avoid unnecessarily lengthy algebra.

Even the quasi-steady case, namely, the interesting limit case as $\omega \rightarrow 0$ does not seem to reduce any substantial amount of algebra and the behavior in this limit is not easy to be studied by a simple inspection.

In the case of a choked cavity, a simple expression for \tilde{g} is obtained as $\omega \rightarrow 0$. From Equations (57) and (58), it is found to be

$$\tilde{g} = \frac{-\frac{1}{\rho} (\tilde{P}_c - \tilde{P}_1) + U \tilde{U}_0 \sqrt{\frac{\Lambda_1 - 1}{\Lambda_1 - c}}}{U \left(1 - \frac{1}{\pi} \sqrt{\frac{\Lambda_1 - 1}{\Lambda_1 - c}} \int_1^0 \sqrt{\frac{c - \xi}{\xi - 1}} \frac{d\xi}{\xi - \Lambda_1} \right)}$$

In our formulation, the complex perturbation velocity was used as the dependent variable. Of course, we might have used the acceleration potential instead. If this had been the case, the boundary conditions would have been non-homogeneous except on the cavity boundary and this fact would have complicated the solution somewhat.

In connection with the present problem, some of the theories on the two-dimensional unsteady cavity flow in an unbounded medium may deserve comments, with the emphasis laid on the highlighted difficulties already mentioned in the general introduction:

Geurst⁽⁵⁾ treated a problem of an unsteady cavitating flat plate held normally to the oncoming flow. He treated the unsteady effects as linear perturbations of the linearized steady flow. His linearized problem was then reduced to a Hilbert problem and a formal solution was obtained. However, there exist two major defects in his formulation. For one thing, he never used the kinematic boundary condition on the cavity surface. Nor did he apply it on any approximate stream surface; instead he completely abandoned it. Secondly, he assumes that there is no source or sink at infinity, which is clearly equivalent to assuming that there is no change in the cavity volume. Some other earlier theories^(6, 7) also adopted either the same assumption or the equivalent assumption that the acceleration potential at infinity be bounded. These assumptions may be valid for certain special flows but its general

application seriously restricts the class of motions a body may perform. Later theories^(8, 9) tried to remove this defect.

Woods⁽⁸⁾ developed a general theory of unsteady cavitation flow past an object in which he allows the singular behavior of the pressure at infinity caused by the source-like effect of the cavity. He assumes that the free material surface enclosing the cavity may be replaced by the stream surface. As he points out, the errors introduced by this assumption may be negligible for slowly varying flows. In his formulation, however, it is uncertain whether the very important kinematic boundary condition has been used at all.

Our present analysis was also based on the assumption that the cavity line may be approximated by the mean stream line which was represented as a straight line in the linearized plane. However, we have explicitly applied the correct kinematic boundary condition on this approximated straight stream line.

Wang and Wu⁽⁹⁾ developed probably the most general theory known thus far in which they included both the condition that the cavity boundary be a material line and an appropriate condition for cavity volume change. They applied the perturbation expansion to the unsteady flow which was assumed to be a small perturbation around some basic steady flow. Similar perturbation analysis might also prove useful for internal flow problems when a rigorous solution is desired. However, a rather involved mathematics will have to be expected in this situation.

As was done in Part I, the problem of Part II has been treated under the assumption that we could separate the unsteady part of the motion completely from the steady part. This assumption is valid only when the change of the cavity length is small. Strictly speaking, the

steady part of all the physical quantities is defined only at points lying within the region of the basic steady flow. Therefore, it was necessary to tacitly assume that the steady part could be continued analytically beyond the original region of the steady flow.

The case of an asymmetric flow will be more complicated to treat for obvious reasons.

In this part of the thesis, the unsteady finite cavity problem in a two-dimensional tunnel with mass fluctuations has been treated and the infinite cavity case was obtained as a limiting problem. Final results should be obtained from numerical calculations. However, the formulation and analysis have been carried out in a self-consistent manner and the solution has been obtained using the complete set of boundary conditions. Also the problem itself is a well-defined representative one for the cavitating internal flow which is of practical interest. Therefore, it is hoped at the moment that the analysis presented herein provides a basis for investigating further complicated cavity problems in internal flows such as cascade flows.

References

1. A. J. Acosta and R. B. Wade, "Experimental Study of Cavitating Hydrofoils in Cascade", California Institute of Technology, Division of Engineering and Applied Science Report, February 1968.
2. C. S. Song, "Vibration of Cavitating Hydrofoils", University of Minnesota, St. Anthony Falls Hydraulic Laboratory Project Report No. 111, October 1969.
3. N. I. Muskhelishvili, Singular Integral Equations, P. Noordhoff Ltd., Gronigen, Holland, 1946.
4. B. R. Parkin, "Linearized Theory of Cavity Flow in Two Dimensions", Rand Corporation Report P-1745, 1959.
5. J. A. Geurst, Linearized Theory of Two-Dimensional Cavity Flows, Thesis, Delft University of Technology, May 3, 1961.
6. T. Y. Wu, "A Linearized Theory for Nonsteady Cavity Flows", California Institute of Technology, Engineering Division Report No. 85-6, September 1957.
7. B. R. Parkin, "Fully Cavitating Hydrofoils in Nonsteady Motion", California Institute of Technology, Engineering Division Report No. 85-2, July 1957.
8. L. C. Woods, "On the Theory of Growing Cavities behind Hydrofoils", Journal of Fluid Mechanics, Vol. 19, 1964.
9. D. P. Wang and T. Y. Wu, "General Formulation of a Perturbation Theory for Unsteady Cavity Flows", Journal of Basic Engineering, Trans. ASME, Series D, Vol. 87, December 1965.
10. F. Sisto, "Linearized Theory of Nonstationary Cascades at Fully Stalled or Supercavitated Conditions", ZAMM 47, 1967.
11. L. C. Woods, "Unsteady Plane Flow past Curved Obstacles with Infinite Wakes", Royal Society of London Proceedings A229, 1955.
12. S. Rubin, "Longitudinal Instability of Liquid Rockets Due to Propulsion Feedback", Journal of Spacecraft and Rockets, Vol. 3, No. 8, August 1966.
13. R. H. Fashbaugh and V. L. Streeter, "Resonance in Liquid Rocket Engine Systems", Trans. ASME, Series D, Vol. 87, December 1965.

14. T. B. Benjamin, "Note on the Interpretation of Two-Dimensional Theories of Growing Cavities", *Journal of Fluid Mechanics*, Vol. 19, 1964.

List of Figure Captions

- Fig. 1(a) Description of the near-cavity field in the tunnel flow
- Fig. 1(b) Sketch showing the general picture of the tunnel flow with cavity viewed as a fluctuating source distribution.
- Fig. 2 Boundary conditions for the linearized flow in the upper half of the tunnel.
- Fig. 3 Boundary conditions in the auxiliary ζ -plane.

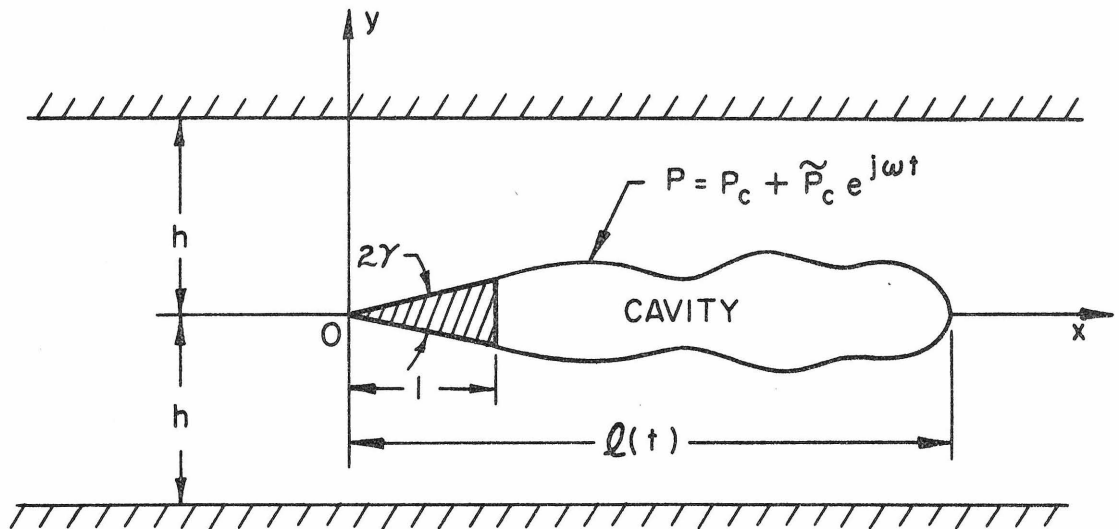


Fig. 1(a) Description of the near-cavity field in the tunnel flow.

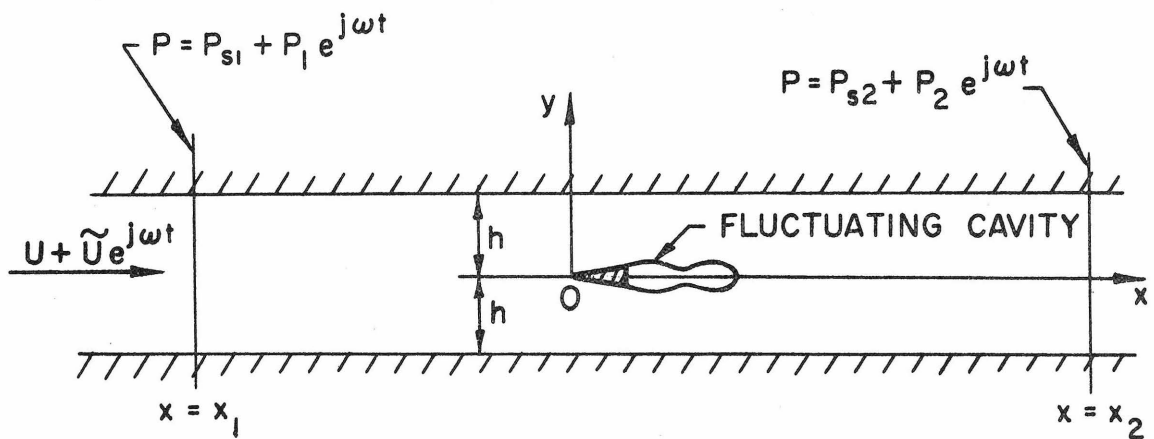


Fig. 1(b) Sketch showing the general picture of the tunnel flow with cavity viewed as a fluctuating source distribution.

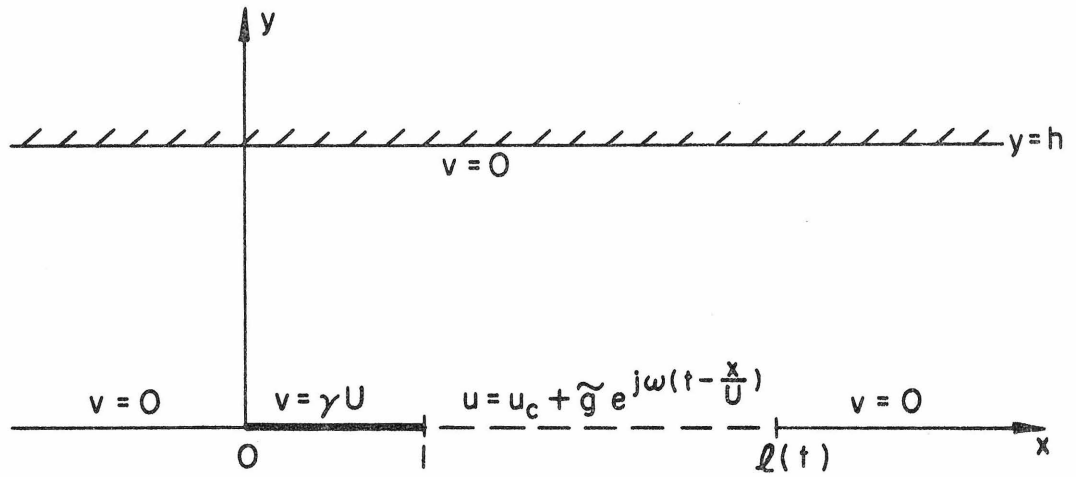


Fig. 2 Boundary conditions for the linearized flow in the upper half of the tunnel.

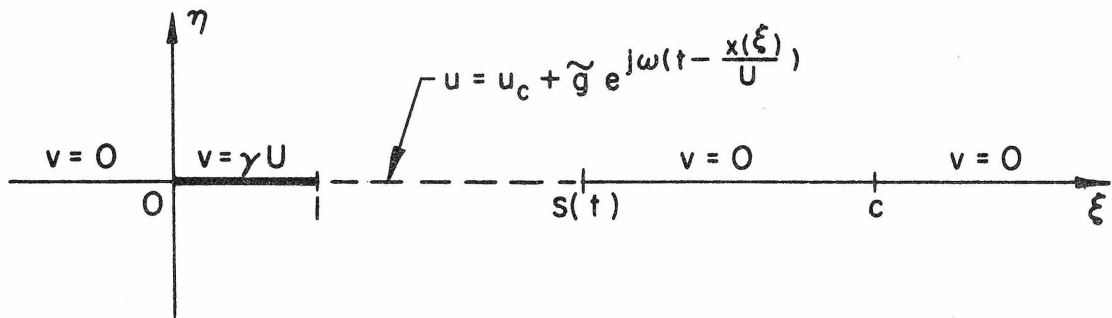


Fig. 3 Boundary conditions in the auxiliary ζ -plane.